Numerical dissipation vs. subgrid-scale modelling for large eddy simulation

Thibault Dairay[a], Eric Lamballais[a], Sylvain Laizet[b], John Christos Vassilicos[b]

[a] *Université de Poitiers, CNRS, ISAE-ENSMA, Institut Pprime, F-86962 Futuroscope Chasseneuil, France*
[b] *Department of Aeronautics, Imperial College London, London SW7 2AZ, United Kingdom*

Abstract

This study presents an alternative way to perform large eddy simulation based on a targeted numerical dissipation introduced by the discretization of the viscous term. It is shown that this regularisation technique is equivalent to the use of spectral vanishing viscosity. The flexibility of the method ensures high-order accuracy while controlling the level and spectral features of this purely numerical viscosity. A Pao-like spectral closure based on physical arguments is used to scale this numerical viscosity *a priori*. It is shown that this way of approaching large eddy simulation is more efficient and accurate than the use of the very popular Smagorinsky model in standard as well as in dynamic version. The main strength of being able to correctly calibrate numerical dissipation is the possibility to regularise the solution at the mesh scale. Thanks to this property, it is shown that the solution can be seen as numerically converged. Conversely, the two versions of the Smagorinsky model are found unable to ensure regularisation while showing a strong sensitivity to numerical errors. The originality of the present approach is that it can be viewed as implicit large eddy simulation, in the sense that the numerical error is the source of artificial dissipation, but also as explicit subgrid-scale modelling, because of the equivalence with spectral viscosity prescribed on a physical basis.

Keywords: Large Eddy Simulation; Subgrid-scale Modelling; Numerical

*Corresponding author.
Email address: eric.lamballais@univ-poitiers.fr (Eric Lamballais)

dissipation; Spectral vanishing viscosity; Pao's spectrum, 3D Taylor-Green flow.

1. Introduction

Thanks to the development of High Performance Computing (HPC), Large Eddy Simulation (LES) has become a widely used technique for the prediction of turbulent flows with a constantly increasing range of applications from fundamental research in fluid mechanics to industrial design (see [1, 2, 3] for an introduction). Despite this favourable situation, LES suffers from weaknesses in its formalism that make some of its results highly questionable.

The traditional presentation of LES is based on the introduction of a low-pass filtering to define the large-scale part of the flow whereas the residual part is referred to as the subgrid-scale (SGS) part. By reference to the common usage, the terminology "subgrid" is used here although the term "subfilter" is more appropriate. The aim of the filter is to reduce the number of degrees of freedom in order to save computational resources by introducing filtered large-scale fields. Governing equations for the large-scale fields can then be established through the introduction of the SGS tensor within the framework of a closure problem. The most restrictive assumption in establishing these equations concerns the commutation between the filtering operator and the spatial derivatives. This point has been addressed in the literature (see for instance [4, 5] and [1, 2] for a review) with the conclusion that a significant error is introduced by this commutation for a distorted computational mesh. Because this error is very difficult to handle, it is almost always ignored through the assumption that it is negligible[1] or included in the subgrid-scale model, both assumptions being equivalent in practical terms.

Another widespread approach to LES is to define the modelling strategy regardless of the numerical errors. This assumption is convenient for developing subgrid-scale models based purely on theoretical and physical arguments. However, it is somewhat disconnected from actual LES practice which is almost entirely based on the use of a marginally refined computational mesh

[1] The commutation error is actually negligible only if the computational mesh distortion is very weak.

in order to save computational time. In Direct Numerical Simulation (DNS), marginal resolution means that the mesh size Δx is close to the Kolmogorov scale η. In LES, the equivalent situation should be that the mesh size Δx is close to the filter size Δ. As recognized by [6], the DNS condition $\Delta x \approx \eta$ is more than enough to ensure accuracy, the reason being that most of the viscous dissipation occurs at scales greater than $O(10\eta)$. Another reason is that at the corresponding wavenumber $\pi k_\eta = \pi/\eta$, the energy spectrum is very steep and the kinetic energy is very low, these two conditions providing a low truncation error for DNS where $\Delta x \approx \eta$. The same cannot be said about LES for which a significant part of the dissipation is ensured by the subgrid-scale model with a substantial truncation error when $\Delta x = \Delta$ as the kinetic energy at the cutoff wavenumber $k = k_\Delta$ (with $k_\Delta = \pi/\Delta$) is still significant. In addition, the kinetic energy spectrum is slowly decreasing at $k \lesssim k_\Delta$. In that particular situation, numerical errors can become prevalent by comparison with the subgrid-scale contribution even with high-order schemes for which the balance between differentiation errors and aliasing errors evolves from the former to the latter.

Even if the role of numerical errors is hardly taken into account in the vast majority of LES carried out on a daily basis, a set of fundamental studies have clearly shown how numerical errors can strongly influence the prediction. For instance, [5, 7] have pointed out through a static analysis that aliasing errors and differentiation errors can be comparable or even outweigh SGS modelling terms in LES under the condition $\Delta x = \Delta$. A simple Fourier analysis can reveal the distortion provided by the numerical discretization [8]. These conclusions have been partially confirmed [9] and also qualified [10] using a model based on two-point turbulence closure. The relative roles of discretization errors and modelling errors have also been investigated directly by LES through *a posteriori* tests as in [11]. Despite the difficulty associated with the definition of a proper criterion for the prediction evaluation, a set of studies (see in particular [12, 13, 14]) has revealed that these two different types of errors can partially cancel each other through a complex interaction, as already suggested in [11]. The resulting error balancing has led to the idea of an optimal choice of the grid resolution vs. the filter length associated with the SGS model while limiting the computational cost. When not connected to a given SGS model like the Smagorinsky model[2], the underlying conclusion

[2]In the Smagorinsky model, only the product of its constant with the filter length is

of these studies (see also [1] chapter 8 for a brief review) is that only the use of mesh size smaller than the filter length allows to control numerical errors in LES through the convergence toward the solution of the model equations. Depending on the order of accuracy of the numerical method, the choice $\Delta/4 \leq \Delta x \leq \Delta/2$ is recommended. While this is a valid recommendation for the reduction of numerical errors in LES, it is almost never followed.

To summarize, the overly restrictive formalism combined with the prevalence of numerical errors leads to a mismatch in LES between practice and theory. Even if most LES users are aware of this mismatch, the conjecture is that it does not seriously affect the results, allowing successful calculations in a wide variety of flow configurations. Naturally, the term "seriously", strongly linked to the goals of the present study, is a matter of debate. This issue is too wide, in relation to the development of verification, validation and quantification of uncertainty techniques in Computational Fluid Dynamics (CFD) [15, 16], and is not addressed in this study. Here, the goal is to examine if this mismatch can be overcome through a more pragmatic approach based on a formalism guided by basic numerical and physical considerations.

LES free of well-defined formalism is not a new concept. It goes back to the development of the MILES approach [17] followed by its varieties more recently referred to as implicit LES [18, 19, 20, 21, 22]. The source of regularisation can come from the discretization of the governing equations but can also be provided by an extra discrete operator that damps [23, 24] or filters [25, 26, 27, 28, 29] selectively the smallest scales. This type of relaxation model can be used alone (see also [30, 31]) or in conjunction with a deconvolution model [32, 33, 34, 35]. For an extensive overview of implicit LES, the reader is referred to the collective book [36] that reflects the diversity of approaches and their connections with explicit SGS modelling.

In this paper, we address the concept of implicit LES in order to propose a favourable balance between numerics and physics, these two features being fully interlinked in implicit LES, as a limitation in terms of physical background but as an advantage from a numerical point of view. How to combine numerics and physical modelling is a key issue for implicit LES. This study is a contribution in this direction in an alternative way where the built-in numerical dissipation does not come from the discretization of the convective term but of the viscous term in the Navier-Stokes equations. It is

meaningful.

shown in this paper that this switch from the convective to the viscous term allows more flexibility in the prescription of the level of numerical dissipation, offering the opportunity to scale it as a conventional SGS model.

The use of the viscous term to introduce numerical dissipation is not harmless if the goal is to mimic SGS modelling because the viscous term is linear whereas the SGS contribution is essentially non-linear. This linear feature prevents any *a priori* direct connection in the physical space between the implicit dissipation and the actual SGS contribution. However, as it will be reported in what follows, it is easy to establish that the discretization error of the viscous term can be viewed as an implicit spectral eddy viscosity. This implicit operator can mimic the expected wavenumber dependence as predicted by two-point closure theories [37, 38, 39] but vanishes at low wavenumbers as required by the numerical consistency. Therefore, despite its essentially linear nature, the artificial dissipation embedded in the viscous term is a valid candidate for implicit functional SGS modelling as any spectral eddy viscosity defined in the Fourier space.

As reported in [36], the most popular implicit LES are based on nonlinear numerical methods through the treatment of advective terms, especially in the general context of nonoscillatory finite volume methods. In this framework, the connection between the nonlinearity of the dissipative numerical methods and the nonlinearity of the actual SGS contribution can even be established through a simplified Modified Equation Analysis (MEA) introduced by [40]. The principle of MEA is to derive the equations whose continuous solution closely approximates the discrete solution of the numerical algorithm corresponding to given numerical schemes. In this particular framework, [41] have shown that the leading truncation error of some non-oscillatory schemes can be expressed in a form similar to an explicit mixed SGS model with a dissipative part and a scale-self-similar part. This connection can be done in a straightforward way in finite-volume differencing because the truncation term takes the form of the divergence of a SGS stress. Then, various schemes and limiters can be classified through their relation to explicit SGS modelling and their expected behaviour in terms of balance between inertial and dissipative contributions. For instance, the lack of scale-self-similar part in implicit SGS modelling is suspected to lead to poor results even when highly accurate numerical methods are used as in [42].

For the present approach where the artificial dissipation comes from the viscous term, the linear nature of the numerical operator excludes de facto any scale-self-similar character of the resulting implicit SGS modelling if not

combined with an explicit SGS model based on a scale-self-similar assumption. However, thanks to its conceptual simplicity, this modelling can be easily expressed in the Fourier space with the *a priori* knowledge of the similarities with spectral SGS models on the full range of scales allowed by the mesh. This is in contrast with MEA where only the asymptotic behaviour of the implicit SGS modelling can be predicted when the mesh size Δx goes to zero. To summarize, even if present linear implicit SGS model is conceptually limited through its lack of any scale-self-similar part, thanks to its simplicity, it offers a Fourier analysis framework where the artificial dissipation can be controlled over the full spectrum of turbulent fluctuations up to the cutoff wavenumber. The association of this favourable feature with an explicit SGS model based on a scale-self-similar assumption (mixed SGS modelling), as it was done for instance by [43] who combined an approximate deconvolution model with SVV, is a natural extension of this work, especially in the context of very large-eddy simulation (VLES).

The view argued in this paper is that the spectral quality of the implicit SGS model, i.e. its relevant scale selectivity for the artificial dissipation introduced, is a very important feature, probably more crucial than the ability to represent the inertial SGS contribution. The successful results presented in what follows clearly support this view for cases where the separation between the explicitly energy containing scales and the modelled scales is significant (typically at least one order of magnitude). Note that this condition on scale separation does not mean that the reduction of the computational cost allowed by the LES is only moderate with respect to DNS. For instance, despite the use of LES mesh that allows us to capture almost 100% of the turbulent kinetic energy, the relative computational effort of present implicit LES with respect to DNS is $1/8^4 \approx 0.024\%$. The corresponding ratio of 8 for the reduction of the LES mesh in every spatial direction by comparison with the DNS mesh is naturally not enough to consider a situation where the cutoff wavenumber belongs to the spectral inertial range. For more critical conditions with a less marked scale separation due to the use of very coarse mesh, the ability of the SGS modelling to mimic the scale-self-similar feature may be more important. This particular category of implicit LES, as distinguished for instance in [21], is out of the scope of the present study.

This study was initiated because of the difficulties experienced by some of the authors to carry out successfully accurate LES using high-order schemes. Conventional subgrid-scale models have been found to be unable to provide solutions free from numerical artefacts using a simple Cartesian solver of the

incompressible Navier-Stokes equations based on high-order finite-difference schemes. For instance, this behaviour is documented in [44] for the LES of a turbulent jet impinging on a heated wall. In that case, eddy viscosity subgrid-scale closures such as the dynamic Smagorinsky [45, 46] or the WALE [47] models were unable to prevent the production of small-scale oscillations. It was observed that these spurious oscillations were highly damaging for the quality of the heat transfer prediction. In the same study, the use of an artificial dissipation was found to improve drastically this prediction through the damping of the small-scale oscillations, leading to smooth solution fields as expected in a formalism based on a filtering procedure. This is one of the paradoxes: a subgrid-scale model used in the classical framework of LES based on filtering cannot in practice ensure the filtering effect under the condition $\Delta x = \Delta$. On the contrary, the use of artificial dissipation, free of rigorous formalism, provides a filtering effect that is beneficial for the accuracy of the calculation. This is a simple illustration of the mismatch between practice and theory in classical LES. As discussed hereinafter, this inability of a conventional subgrid-scale model to control spurious small-scale oscillations is mainly related to the condition $\Delta x = \Delta$ which is clearly against the numerical accuracy.

As high-order methods progress in CFD, especially for spectral/hp element approaches [48, 49], this inability of classical LES to control spurious small-scale oscillation is regularly observed. To overcome this weakness, a selective action on the smallest scales is often carried out. This selective action can be based on a numerical stabilisation procedure (see for instance [50, 51, 52, 53, 54, 55, 56, 57] for the use of spectral vanishing viscosity, of particular interest in this study) that can be combined with a more sophisticated subgrid-scale model, in particular in the context of Variational Multiscale (VMS) methods [58, 59, 60, 61]. When these two actions are combined, depending on the numerical parameters driving the regularisation, more or less weight on the physical subgrid-scale model can be added.

In this work, we address the basic question of numerical dissipation vs. subgrid-scale modelling. For that purpose, a Cartesian code is used to solve the 3D Taylor-Green problem using a regular grid to mesh the triperiodic cubic computational domain. The spatial differentiation is based on compact finite difference schemes with well-known accuracy and stability properties. The schemes are purely centred, and the artificial dissipation is introduced via the viscous term in a controlled way. The code ensures the kinetic energy conservation (in the limit of zero time discretization error and viscosity), as

is also the case of more multi-purpose robust CFD codes based on high-order schemes.

The physics of the 3D Taylor-Green problem should not be viewed as a simple turbulent LES benchmark as it requires to handle correctly the complete transition process (destabilization phase and 3D breakdown) followed by the establishment of fully developed turbulence decaying in time. The interest of this demanding benchmark in LES has already been shown by [62, 63, 64, 29, 65, 66, 67]. To make it more challenging and representative of realistic turbulence, two high values of Reynolds number are considered here using highly-resolved DNS results as a reference for the assessment of their LES counterparts.

In addition to the comparison between numerical dissipation and explicit subgrid-scale modelling, a new way to calibrate the former on the latter (i.e. through a physical scaling) is also presented in the paper. Thanks to its physical input, the numerical dissipation becomes a substitute subgrid-scale model making the distinction between artificial dissipation and subgrid-scale modelling less meaningful. The same can be said about the classification between conventional LES based on explicit subgrid-scale modelling and implicit LES, this classification becoming less obvious if the "implicit" dissipation is controlled "explicitly". In this work, the notion of "controlled implicit LES" is introduced, "implicit" because the extra-dissipation corresponds to numerical errors and "controlled" because the level of these errors is chosen on a physical basis.

2. Numerical methodology

2.1. Governing equations

As already mentioned in the introduction, an academic flow configuration is considered with the aid of a high-order code. The massively parallel code Incompact3d is used to solve the incompressible Navier-Stokes equations

$$\frac{\partial u_i}{\partial t} + \frac{1}{2}\left(u_j\frac{\partial u_i}{\partial x_j} + \frac{\partial u_i u_j}{\partial x_j}\right) = -\frac{1}{\rho}\frac{\partial p}{\partial x_i} + \nu\frac{\partial^2 u_i}{\partial x_j \partial x_j} - \frac{\partial \tau_{ij}}{\partial x_j} \quad (1)$$

$$\frac{\partial u_i}{\partial x_i} = 0 \quad (2)$$

where $p(x_j,t)$ is the pressure field (for a fluid with a constant density ρ), $u_i(x_j,t)$ the velocity field, ν the kinematic viscosity and τ_{ij} are subgrid-scale (SGS) stresses associated with the use of an explicit SGS model.

Note that for the present approach, no reference to any filter is explicitly written in the equations, except that the filter needs to be homogeneous in space. However, when solved in LES mode with or without explicit SGS model, the unknowns u_i and p should be interpreted as the large-scale component of velocity and pressure through the separation scale Δ.

2.2. General description of the code

The code Incompact3d is based on compact sixth-order finite difference schemes for the computation of interpolation, first and second derivatives. The mesh is Cartesian in a half-staggered arrangement meaning that the nodes are the same for the three velocity components while being half-staggered for the pressure. This particular mesh organisation requires mid-point operators for interpolation and first derivative but only for the treatment of the pressure and incompressibility. Every finite-difference operator is purely centred with, except for the calculation of second derivatives and interpolation, an optimal reduced stencil preserving the sixth-order accuracy as described by [68]. For a more detailed presentation of the code Incompact3d, the reader is referred to [69, 70, 71] where all its numerical schemes are clearly defined as well as its features for massively parallel computing.

The reason for using a scheme with an extended stencil to compute the second derivatives in the viscous term is explained in subsection 2.4. The choice to also use a slightly extended stencil for mid-point interpolator associated with the half-staggered mesh arrangement is less crucial. In preliminary calculations, it was observed that when an explicit subgrid-scale model is used with $\Delta = \Delta x$, the use of a "quasi-spectral" scheme (as designated by [68]) for mid-point interpolation improves the results while having no significant effect when numerical dissipation is used. The sensitivity of results to mid-point interpolation is related to the presence of spurious oscillations at the mesh size. Here, this improved interpolation scheme has been used in order to put the explicit subgrid-scale modelling that we used (in effect the Smagorinsky model) in the most favourable situation possible thus enabling general conclusions from our comparisons. Its transfer function is compared to the classic scheme (optimal stencil for sixth-order accuracy) in figure 1-left. Its ability to ensure $T_f(k) \approx 1$ on a wide range of wavenumbers leads to a better treatment of the incompressibility condition. More details about the selection of the corresponding scheme coefficients can be found in [68].

The convective term in equation (1) is written in the skew-symmetric form as it is actually computed in the code. This specific form is known to reduce

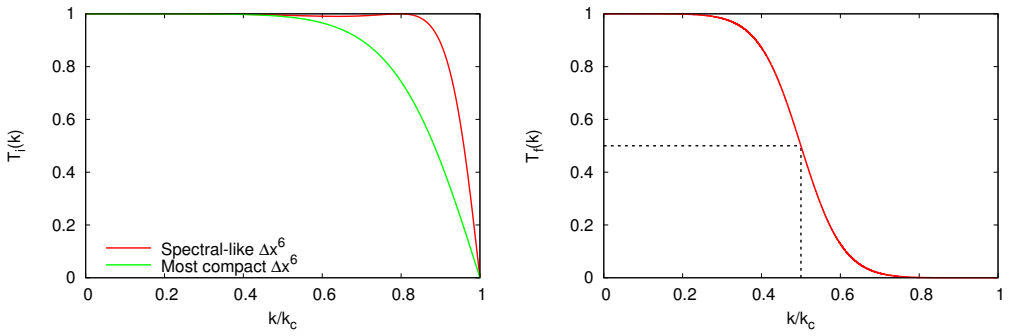

Figure 1: Transfer function associated with the finite-difference sixth-order mid-point interpolation (left) and test filter (right) with $\hat{f}(k) = T_i(k)f(k)$ and $\tilde{f}(k) = T_f(k)f(k)$ respectively when expressed in the Fourier space.

aliasing errors [72]. One more important feature of the skew-symmetric form is that it enables the present code to ensure the kinetic energy conservation in the inviscid limit up to time discretization errors. This property, assessed practically for the present flow configuration, will be shown in the next section. This is an attractive feature in the sense that only the discrete viscous operator is responsible for kinetic energy dissipation when $\tau_{ij} = 0$, as in the continuous case. This is in contrast with the most popular methods in implicit LES where the artificial dissipation is introduced by upwind schemes for the differentiation of the convective term. This clear distinction between the contributions from the convective and viscous terms combined with the flexibility in the control of the numerical dissipation related to the latter is one of the advantages of the present approach.

2.3. Explicit SGS modelling

In this study, two reference SGS models have been tested for comparison with the present approach based on numerical dissipation. The first model is the very popular standard Smagorinsky model [45] with

$$\tau_{ij} = -2\left(C_s\Delta\right)^2 |S| S_{ij} \tag{3}$$

where

$$S_{ij} = \frac{1}{2}\left(\frac{\partial u_i}{\partial x_j} + \frac{\partial u_j}{\partial x_i}\right) \tag{4}$$

is the strain rate tensor and $|S|$ its magnitude with $|S| = \sqrt{2S_{ij}S_{ij}}$. In this model, to characterize the filtering effect, only the product of the model constant C_s by the model filter size Δ is actually meaningful. Here, a single value $C_s = 0.1$ will be considered for a reason explained hereinafter.

The dynamic version of the Smagorinsky model [46, 73] simply means here that C_s is estimated dynamically through a well-known procedure based on the Germano identity. The flow configuration considered in this work allows the use of a simple and robust version of this procedure [74] where $C_s(t)$ depends only on time with

$$C_s^2(t) = \frac{\left\langle \mathcal{M}_{ij}\left(\mathcal{L}_{ij} - \frac{1}{3}\mathcal{L}_{kk}\delta_{ij}\right)\right\rangle}{\langle \mathcal{M}_{kl}\mathcal{M}_{kl}\rangle} \tag{5}$$

where $\langle . \rangle$ denotes a spatial averaging over the entire computational domain. Both $\mathcal{L}_{ij}$ and $\mathcal{M}_{ij}$ are based on the definition of a test filter $\widetilde{(.)}$ of size $\tilde{\Delta}$ with

$$\mathcal{L}_{ij} = \widetilde{u_i u_j} - \tilde{u}_i \tilde{u}_j \tag{6}$$

and

$$\mathcal{M}_{ij} = 2\Delta^2 \widetilde{|S|S_{ij}} - 2\tilde{\Delta}^2 |\tilde{S}|\tilde{S}_{ij} \tag{7}$$

Note that thanks to the averaging operator $\langle . \rangle$, no negative value of C_s^2 has been obtained, consistently with its positive definition. As test filter size, the robust and very common choice $\tilde{\Delta} = 2\Delta$ has been chosen. Because the test filter must be applied explicitly, an extra finite-difference operator has been used. As for the other discretization operators in the code Incompact3d, a compact sixth-order order formulation has been used with a transfer function shaped to fall down at $k \approx k_c/2$ consistently with the choice $\tilde{\Delta} = 2\Delta$. The resulting transfer function is illustrated in figure 1-right.

2.4. Numerical dissipation through the approximation of the viscous term

Because the scheme used to estimate the second derivatives in the present study is not too conventional, a detailed description is given in this subsection. As a centred compact finite difference scheme, a $3-9$ stencil formulation is used with

$$\begin{aligned} \alpha f''_{i-1} + f''_i + \alpha f''_{i+1} &= a\,\frac{f_{i+1} - 2f_i + f_{i-1}}{\Delta x^2} + b\,\frac{f_{i+2} - 2f_i + f_{i-2}}{4\Delta x^2} \\ &+ c\,\frac{f_{i+3} - 2f_i + f_{i-3}}{9\Delta x^2} + d\,\frac{f_{i+4} - 2f_i + f_{i-4}}{16\Delta x^2} \end{aligned} \tag{8}$$

where $f_i = f(x_i)$ and $f''_i = f''(x_i)$ denote the values of the function $f(x)$ and its second derivatives $f''(x)$ at the nodes $x_i = (i-1)\Delta x$ and where Δx is a uniform mesh spacing. It is a 5 coefficients (α, a, b, c, d) scheme for which a single combination can ensure tenth-order accuracy. Because sixth-order accuracy is expected in the present code, two coefficients can be freely chosen if the three following constraints are preserved: (i) $a + b + c + d = 1 + 2\alpha$ (Δx^2 condition); (ii) $a + 4b + 9c + 16d = 12\alpha$ (Δx^4 condition); (iii) $a + 16b + 81c + 256d = 30\alpha$ (Δx^6 condition).

A well-known way to analyse the resolution properties of finite-difference schemes is to consider their behaviour in Fourier space where a modified square wavenumber k'' can be associated with the scheme (8) with

$$k''(k) = \frac{\begin{array}{c} 2a\left[1-\cos(k\Delta x)\right] + \frac{b}{2}\left[1-\cos(2k\Delta x)\right] + \\ \frac{2c}{9}\left[1-\cos(3k\Delta x)\right] + \frac{d}{8}\left[1-\cos(4k\Delta x)\right] \end{array}}{\Delta x^2\left[1+2\alpha\cos(k\Delta x)\right]} \tag{9}$$

where $k \in [0, k_c]$ is the actual wavenumber and $k_c = \pi/\Delta x$ is its cutoff value associated with the mesh. A remarkable feature of this expression is that it can become singular at $k = k_c$ when $\alpha = 1/2$. The resulting strong overestimation of the second derivative at $k \approx k_c$ when $\alpha \to 1/2$ has led [75] to suggest an alternative method to introduce a controlled high-order numerical dissipation for a negligible extra computational time.

To adequately characterise the extra-dissipation introduced by a given set of coefficients, it is useful to introduce the associated spectral viscosity defined as

$$\nu''_s(k) = \nu\frac{k'' - k^2}{k^2} \tag{10}$$

This expression can be used to adjust the coefficients (α, a, b, c, d) in order to mimic an hyperviscous kernel [76, 77, 78] or a Spectral Vanishing Viscosity (SVV) kernel [79, 80, 81, 53] as shown initially by [75] and more recently by [44] for the sixth-order accurate scheme (8). In this work, the coefficient adjustment will be made by reference with the SVV that reads

$$\nu_s(k) = \begin{cases} 0 & \text{if } k < mk_c \\ \nu_0 \exp\left[-\left(\frac{k_c - k}{mk_c - k}\right)^2\right] & \text{if } mk_c \le k \le k_c \end{cases} \tag{11}$$

where ν_0 is a parameter controlling the value of the spectral viscosity at the cutoff whereas $\nu_s(k)/\nu_0$ gives the shape of the kernel. The sensitivity to the

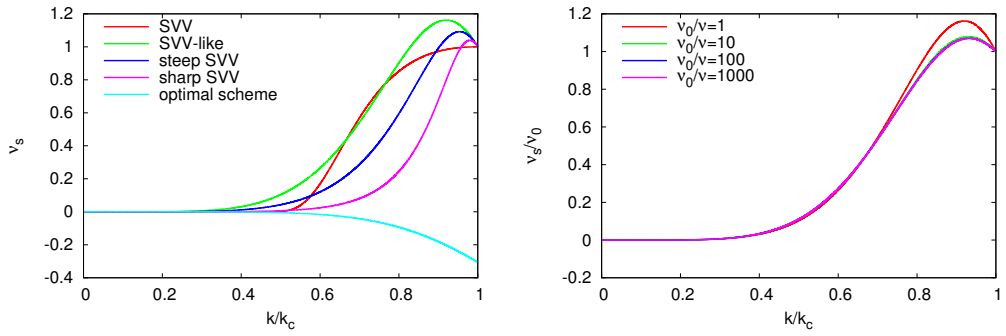

Figure 2: Left: SVV-like, steep and sharp SVV kernels when $\nu_0/\nu = 1$ and for the optimal scheme (12) that imposes $\nu_0/\nu \approx -0.3$. Right: sensitivity of SVV-like kernel to ν_0/ν (similar behaviour for the steep and sharp SVV kernel not shown).

control parameters of SVV has been investigated by [51], in particular to the parameter m defining its scale selectivity. In this study, the standard SVV corresponds by convention to the intermediate value $m = 0.3$. Because the five parameters (α, a, b, c, d) are only subjected to three conditions to ensure sixth-order accuracy, two additional conditions can be imposed to obtain the same spectral viscosity at the cutoff and at a second wavenumber in order to shape the kernel. In [44], this second wavenumber was chosen at $k = 2k_c/3$, leading to the two extra conditions : (iv) $k''(k_c) = (1 + \nu_0/\nu)k_c^2$; (v) $k''(2k_c/3) = (1 + c_1\nu_0/\nu)4k_c^2/9$ with $c_1 \approx 0.44$ as given by the SVV kernel (11) at $k = 2k_c/3$.

The ability of scheme (8) to provide a kernel close to the SVV one as given by (11) is illustrated in figure 2-left with the arbitrary choice $\nu_0 = \nu$. Using the coefficient relations provided by [44], a SVV-like kernel can be obtained for which the spectral viscosity is applied on a wide range of wavenumbers. In order to reduce this range with a better fit of the vanishing property of the SVV, a steep and sharp kernel are also presented in figure 2-left where condition (v) was imposed using $c_1 = 0.22$ and 0.055 respectively.

One remarkable feature of this way to adjust the scheme coefficient is that any value of ν_0 can be imposed while keeping almost constant the associated kernel. This feature is illustrated in figure 2-right for $\nu_0/\nu = 1, 10, 100$ and 1000. In addition, thanks to the singularity in expression (9) when $\alpha \to 1/2$, a very sharp kernel can be used, making the adjustment method very flexible for applying numerical dissipation at the desired level on the desired range of scales in the neighbourhood of the cutoff wavenumber k_c.

It is worth mentioning that this extra dissipation provided by the overestimation of the second derivative is not a "natural" property of the general scheme (8), in particular when the coefficients are chosen to be optimal in terms of stencil reduction and accuracy order. For instance, the well-known $3-5$ stencil formulation can offer the sixth-order accuracy (see [68]) through the choice

$$(\alpha, a, b, c, d) = (2/11, 12/11, 3/11, 0, 0) \tag{12}$$

in the scheme (8), making it more compact. This very popular scheme is accurate on a wide range of scales but significantly underestimates the second derivative near the cutoff wavenumber. It is easy to show that this underestimation corresponds to an underdissipative feature with an associated negative spectral viscosity $\nu_s'' < 0$ that is maximum in absolute value at $k = k_c$ with $\nu_s''(k_c) = \nu_0$ and $\nu_0/\nu = (48/7 - \pi^2)/\pi^2 \approx -0.3$. The resulting negative kernel, plotted in figure 2-left, reduces the ability of the viscous term to control spurious oscillations at small scale. In this study, this conventional scheme is used as a reference with the conclusion that a controlled overdissipative behaviour through a positive value of ν_0 is highly preferable.

The flexibility in the prescription of $\nu_s''(k)$ can also be seen as a drawback because of the arbitrariness introduced by the need to choose both ν_0 and the kernel $\nu_s''(k)/\nu_0$ appropriately case by case. In the next section, a simplified spectral closure is proposed as a tool to constrain this choice by an appropriate physical scaling of the numerical dissipation.

3. Pao-like closure for the scaling of numerical dissipation

In the framework of homogeneous and isotropic turbulence, the Lin equation for the spectral density of kinetic energy $E(k,t)$ holds with

$$\frac{\partial E(k,t)}{\partial t} = T(k,t) - 2\nu k^2 E(k,t) \tag{13}$$

where k and t are the wavenumber and the time respectively whereas $T(k)$ is the transfer term related to the energy flux $\Pi(k)$ by $-d\Pi(k)/dk = T(k)$. In the inertial spectral range where the Kolmogorov equilibrium theory assumes the energy spectrum to be effectively stationary [82] the Lin equation simplifies to

$$T(k) = 2\nu k^2 E(k). \tag{14}$$

To obtain an *a priori* form of the energy flux, Pao [83] suggests to visualise the migration of a spectral unit of energy from k at the time[3] τ to $k+\delta k$ at the time $\tau+\delta\tau$. This view leads to the definition of the velocity $\sigma(k)$ of the spectral unit in the wavenumber space with

$$\sigma(k) = \frac{dk}{d\tau} \tag{15}$$

so that the flux of energy across k can also be written

$$\Pi(k) = E(k)\sigma(k). \tag{16}$$

As in the Kolmogorov theory [84], this flux can be assumed to depend only on the dissipation

$$\varepsilon = \int_0^\infty 2\nu k^2 E(k) dk \tag{17}$$

and the wavenumber k. Then, for dimensional reasons, $\sigma(k)$ must be expressed as

$$\sigma(k) = C_1 \varepsilon^{1/3} k^{5/3} \tag{18}$$

leading to

$$\Pi(k) = C_1 \varepsilon^{1/3} k^{5/3} E(k). \tag{19}$$

The combination of this expression with equation (14) leads to the differential equation

$$\frac{d}{dk}\left(C_1 \varepsilon^{1/3} k^{5/3} E(k)\right) + 2\nu k^2 E(k) = 0 \tag{20}$$

which provides the analytical solution

$$E(k) = C_2 k^{-5/3} \exp\left(-\frac{3}{2}\frac{\nu k^{4/3}}{C_1 \varepsilon^{1/3}}\right). \tag{21}$$

The two constants C_1 and C_2 can be related to each other by using (17), and connecting (21) with the Kolmogorov spectrum leads to the final expression

$$E(k) = C_k \varepsilon^{2/3} k^{-5/3} \exp\left(-\frac{3}{2} C_k \left(\frac{k}{k_\eta}\right)^{4/3}\right) \tag{22}$$

[3] The stationarity still holds, this is just a way to describe the statistically stationary energy cascade process.

where $k_\eta = \varepsilon^{1/4}/\nu^{3/4}$ is the Kolmogorov wavenumber and C_k the Kolmogorov constant (see [83] for more details).

A similar approach can be used to predict the influence of the present numerical dissipation on the spectrum by simply replacing k^2 on the right hand side of equation (20) with $k''(k)$ as given by expression (9). Of course, such an approach assumes the validity of Kolmogorov's statistical stationarity assumption which we know is not valid in unsteady turbulent flows such as the one studied here (see [85]). However, this is a first attempt at designing a tool for predicting the influence of our model's numerical dissipation on the spectrum and it is reasonable to base it on Kolmogorov's well-established equilibrium framework. Non-equilibrium modifications will follow in future works.

Fortunately, it is easy and computationally inexpensive to solve numerically equation (20) with $k''(k)$ given by (9), i.e.

$$\frac{d}{dk}\left(\frac{1}{C_k}\varepsilon^{1/3}k^{5/3}E(k)\right) + 2\nu k''(k)E(k) = 0 \tag{23}$$

which also reads

$$\frac{dE(k)}{dk} + \left(\frac{5}{3k} + \frac{2C_k k''(k)}{k_\eta^{4/3}k^{5/3}}\right)E(k) = 0. \tag{24}$$

In practice, equation (24) is solved by integration from the wavenumber k_s to any wavenumber $k > k_s$ using the Pao solution as boundary condition at $k = k_s$, i.e.

$$E(k_s) = C_k\varepsilon^{2/3}k_s^{-5/3}\exp\left(-\frac{3}{2}C_k\left(\frac{k_s}{k_\eta}\right)^{4/3}\right). \tag{25}$$

To be compatible with the Pao assumptions, k_s must be chosen in the inertial range. Another restriction is that the condition $k''(k_s) = k_s^2$ must be ensured for consistency with (25). This condition, corresponding to $\nu_s''(k_s) = 0$, is automatically ensured using the SVV kernel (11) provided that $k_s < 0.3k_c$. For the present approach where the kernel is given by (10) using (9), the more restrictive relation $k_s = k_c/8$ has been used to check accurately the approximate condition $k''(k_s) \approx k_s^2$.

Interestingly, the Pao-like solutions of equation (24) all lead to the same partial dissipation $\varepsilon_{>k_s}$

$$\varepsilon_{>k_s} = \int_{k_s}^{\infty} 2\nu k''(k)E(k)dk \tag{26}$$

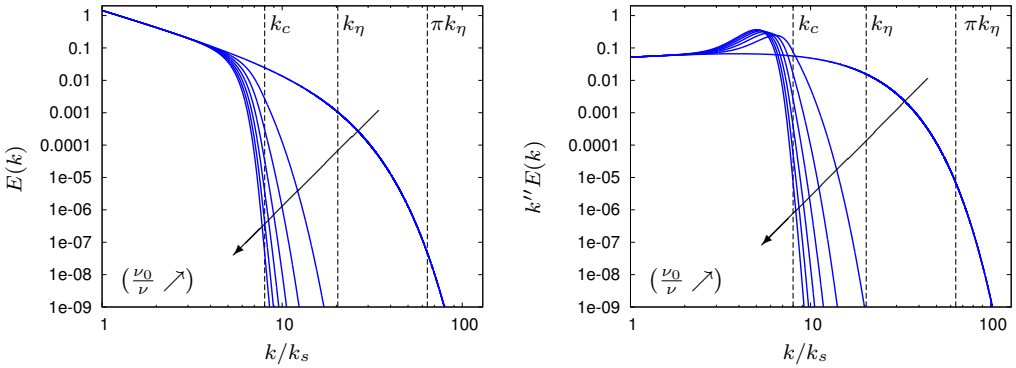

Figure 3: Kinetic energy $E(k)$ and dissipation $k''E(k)$ spectra obtained by solving the Pao-like equation from $\nu_0/\nu = 0$ (reference Pao solution) to $\nu_0/\nu = 66$ by steps of 11. Case with $\pi k_\eta/k_c = 8$ using the steep SVV kernel.

provided that they have the same behaviour at the integral boundaries. This can be shown by integration of equation (23) from k_s to ∞ while using the boundary condition (25) that leads to

$$\begin{aligned} \varepsilon_{>k_s} &= -\left[\frac{1}{C_k}\varepsilon^{1/3}k^{5/3}E(k)\right]_{k_s}^{\infty} \\ &= \varepsilon \exp\left(-\frac{3}{2}C_k\left(\frac{k_s}{k_\eta}\right)^{4/3}\right). \end{aligned} \tag{27}$$

for any $k''(k)$, i.e. for any kernel $\nu_s''(k)/\nu_0$ and any value ν_0.

The numerical solver of the Pao-like equation (24) is a very simple and computationally inexpensive model that offers a straightforward prediction of the influence of the present numerical dissipation on the kinetic energy spectrum $E(k)$. The prediction can be done for any value of ν_0 and any kernel of spectral viscosity $\nu_s''(k)/\nu_0$. This ability is illustrated in figure 3 using a SVV-like kernel. Six Pao-like solutions are presented in order to observe how the increase of ν_0/ν modifies the kinetic energy spectrum and its related dissipation spectrum that includes the numerical contribution. The reference spectrum corresponds to the case $\nu_0/\nu = 0$ for which the Pao spectrum (22) is virtually recovered. Then, ν_0/ν is increased by steps of 11 up to the value 66. As ν_0/ν is increased, the overall range of the predicted spectrum is reduced. For the highest values of ν_0/ν, this reduction corresponds to a strong fall at the cutoff wavenumber $k_c/k_s = 8$.

In the simplified framework of this present spectral closure, the conventional Pao spectrum corresponds to what should be obtained from a DNS based on a discretization $\Delta x = \eta$ in order to capture accurately the viscous range of the spectrum. Such a mesh size corresponds to a cutoff wavenumber of πk_η for which $E_{DNS}(\pi k_\eta)$ is very low, this condition allowing the assumption that the truncation error is small enough to ensure the numerical convergence expected for DNS. If the same numerical point of view is adopted for the highest value $\nu_0/\nu = 66$ presented in figure 3, it can be assumed that a mesh size $\Delta x = \pi/k_c$ is enough thanks to the corresponding low level of $E(k_c)$ that is close to $E_{DNS}(\pi k_c)$. Since the Pao-like spectra can be assumed to correspond to LES spectra obtained with different levels of numerical dissipation, a reasonable choice of ν_0/ν is to adjust its value in order to get the same kinetic energy at k_c as at πk_η for the reference DNS, namely

$$E_{LES}(k_c) = E_{DNS}(\pi k_\eta) \tag{28}$$

where $E_{DNS}(k)$ refers to the Pao spectrum obtained at $\nu_0 = 0$ whereas $E_{LES}(k)$ corresponds to the predicted solution of the Pao-like solver at a given value of ν_0/ν.

In the example illustrated in figure 3, a simple dichotomic search provides the value $\nu_0/\nu = 63.08$. Thanks to the negligible computational cost of the numerical Pao-like solver, this dichotomic search based on condition (28) can be performed extensively for any ratio $\pi k_\eta/k_c$. Figure 4 presents the resulting behaviour for the range $1 \leq \pi k_\eta/k_c \leq 16$. As expected, the steep and sharp SVV kernels (that are also "more vanishing" at small wavenumber as plotted in figure 2-left) require to use significantly higher values of ν_0/ν (see figure 4) to ensure condition (28).

Figure 3-right presents the dissipation spectra associated with the Pao-like solutions. It can be observed how the use of the present high-order numerical viscosity can concentrate an extra-dissipation near $k \lesssim k_c$ in order to compensate the lack of dissipation for $k > k_c$ due to the strong fall of the kinetic energy spectrum. Naturally, this lack of dissipation beyond k_c is an advantage because it could not be taken into account using a discretization based on mesh size with $\Delta x = \pi/k_c$. Its compensation through the extra-dissipation near $k \lesssim k_c$ is a feature of the present spectral closure that automatically ensures a constant value for $\varepsilon_{>k_s}$ through the connection with the Pao solution at $k = k_s$ as shown by equation (27). In a practical calculation, this connection between the LES and DNS spectra at $k = k_s$ is

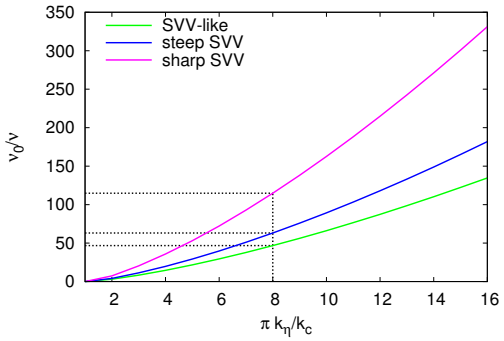

Figure 4: Evolution of ν_0/ν with $\pi k_\eta/k_c$ to ensure $E_{LES}(k_c) = E_{DNS}(\pi k_\eta)$ as predicted by the Pao-like solver.

not guaranteed as well as the compensation mechanism that keeps constant the full dissipation including its artificial component. How a LES actually reacts to the application of the numerical dissipation, by comparison to the prediction of this very simple model and also by comparison to classical SGS models, is the main subject of the rest of this paper.

4. Results

4.1. Flow configuration and numerical parameters

As already mentioned, the 3D Taylor-Green vortex problem is chosen to compare the two main LES strategies based on either numerical dissipation or on explicit subgrid-scale modelling. As a trade-off, the numerical dissipation is chosen according to the prediction of ν_0/ν from the Pao-like solver presented in the previous section.

In the Taylor-Green problem, the solution is subjected to periodicity in the three directions of space in a cubic computational domain of size $(2\pi)^3$. The initial condition, simply composed of one different Fourier mode on two velocity components

$$\begin{aligned} u(x_i,0) &= \sin(x)\cos(y)\cos(z) \\ v(x_i,0) &= -\cos(x)\sin(y)\cos(z) \\ w(x_i,0) &= 0 \end{aligned} \tag{29}$$

leads to a strongly non-linear evolution of the flow toward a fully developed turbulent state. This is a decaying turbulence problem in terms of kinetic

energy

$$E_k = \frac{1}{(2\pi)^3} \int_{(2\pi)^3} \frac{u_i u_i}{2} d\mathbf{x}^3 \tag{30}$$

that is related to dissipation

$$\varepsilon = \frac{1}{(2\pi)^3} \int_{(2\pi)^3} \nu \frac{\partial u_i}{\partial x_j} \frac{\partial u_i}{\partial x_j} d\mathbf{x}^3 \tag{31}$$

with the simple equation

$$\frac{dE_k}{dt} = -\varepsilon. \tag{32}$$

The transition processes result in a strong peak of enstrophy

$$\zeta = \frac{1}{(2\pi)^3} \int_{(2\pi)^3} \frac{\omega_i \omega_i}{2} d\mathbf{x}^3 \tag{33}$$

due to vortex stretching mechanisms that amplify in average the modulus of the vorticity components ω_i. This first stage is followed by a constant decay of enstrophy where a turbulent cascade subjected to viscous effects can be observed. In the present triperiodic domain, it is easy to show that dissipation and enstrophy are directly related by the algebraic relation

$$\zeta = 2\nu\varepsilon \tag{34}$$

For more details about the Taylor-Green vortex problem, see [86].

For the purpose of the present investigation, two DNS have been performed at Reynolds numbers $Re = 1/\nu$ sufficiently high to allow the development of a wide range of turbulent scales making more meaningful a LES approach where the small-scales discarded from the explicit calculation should not be mainly located in the viscous range of the kinetic energy spectrum. The two values considered $Re = 5000, 10000$ require a significant computational effort with the need of 1280^3 and 2048^3 of mesh points respectively to discretize the cubic domain $(2\pi)^3$ while ensuring the expected DNS accuracy. Here, to reduce the computational cost, we have used in part the symmetries of the Taylor-Green vortex problem that enable us to calculate the flow only inside the impermeable box π^3 with a reduction by 8 of the number of degrees of freedom. However, for reasons of consistency with previously documented results and to avoid any confusion, all the spatial resolutions are given by reference to the full cubic domain $(2\pi)^3$.

In this study, DNS results are only used as a reference to assess the quality of the various types of LES. The main parameters of all calculations are summarized in table 1. Calculations 1 and 15 are the reference DNS. Calculation 0 has been obtained with $\nu = 0$ and $\tau_{ij} = 0$, meaning that the Euler equations are solved with the code Incompact3d using the same numerical parameters as the LES at $Re = 5000$ but without imposing symmetries in order to enable the solution to eventually transform into a homogeneous white noise. Calculations 2 and 16 are LES without any SGS modelling (neither explicit nor implicit) using the conventional under-dissipative scheme given by the coefficients (12) in (8) for the computation of the viscous term. Calculations 3–6 and 17–19 correspond to LES performed using the values ν_0/ν predicted by the Pao-like solver for the ratio $\pi k_\eta/k_c = 8$ and the three SVV kernels examined (SVV-like, steep SVV, sharp SVV). Calculations 7–10 and 11–14 have been performed to consider the numerical convergence of the standard and dynamic Smagorinsky models. A specific convergence of the numerical dissipation will also be discussed using calculations 4 and 5. Calculations 7, 11, 20 and 21 correspond to the classical usage of these two SGS models through the condition $\Delta x = \Delta$.

4.2. Time evolution of the kinetic energy

The time evolution of $E_k(t)$ and its related dissipation ε_t are plotted in figure 5 for the DNS and LES free of explicit modelling at the two Reynolds numbers considered. The kinetic energy is estimated through an averaging over the mesh nodes of the entire computational grid, namely $E_k = \langle u_i u_i \rangle /2$ consistently with definition (30). The related total dissipation $\varepsilon_t(t)$ is estimated by time differentiation of $E_k(t)$ with $\varepsilon_t = -dE_k/dt$ as in relation (32). It has been checked that $\varepsilon_t \approx \varepsilon$ for the two DNS where $\varepsilon = \nu \left\langle \frac{\partial u_i}{\partial x_j} \frac{\partial u_i}{\partial x_j} \right\rangle$ as in the definition (31) based on first derivatives. In addition, for this first series of calculations free from explicit subgrid-scale modelling, it has also been checked that ε_t is virtually identical to its alternative estimation based on second derivatives with $\varepsilon_t = -\nu \left\langle u_i \frac{\partial^2 u_i}{\partial x_j \partial x_j} \right\rangle$. This almost perfect agreement simply means that the kinetic energy conservation is correctly ensured by the convective terms at the discrete level. This conservation property is directly illustrated in figure 5 for calculation 0 (inviscid case) for which E_k keeps its initial value up to the end of the simulation where velocity fluctuations look like a white noise.

Name	Type	SGS model	Re	n_x	Δx	Δ
0	Euler	–	∞	160	0.0392	–
1	DNS	–	5000	1280	0.0049	–
2	LES	–	5000	160	0.0392	–
3	LES	SVV-like, $\nu_0/\nu = 47$	5000	160	0.0392	–
4	LES	steep SVV, $\nu_0/\nu = 63$	5000	160	0.0392	–
5	LES	steep SVV, $\nu_0/\nu = 63$	5000	320	0.0196	–
6	LES	sharp SVV, $\nu_0/\nu = 115$	5000	160	0.0392	–
7	LES	standard Smagorinsky	5000	160	0.0392	0.0392
8	LES	standard Smagorinsky	5000	320	0.0196	0.0392
9	LES	standard Smagorinsky	5000	480	0.0131	0.0392
10	LES	standard Smagorinsky	5000	640	0.0098	0.0392
11	LES	dynamic Smagorinsky	5000	160	0.0392	0.0392
12	LES	dynamic Smagorinsky	5000	320	0.0196	0.0392
13	LES	dynamic Smagorinsky	5000	480	0.0131	0.0392
14	LES	dynamic Smagorinsky	5000	640	0.0098	0.0392
15	DNS	–	10000	2048	0.0031	–
16	LES	–	10000	256	0.0245	–
17	LES	SVV-like, $\nu_0/\nu = 47$	10000	256	0.0245	–
18	LES	steep SVV, $\nu_0/\nu = 63$	10000	256	0.0245	–
19	LES	sharp SVV, $\nu_0/\nu = 115$	10000	256	0.0245	–
20	LES	standard Smagorinsky	10000	256	0.0245	0.0245
21	LES	dynamic Smagorinsky	10000	256	0.0245	0.0245

Table 1: Main parameters of the calculations. As the present computational grid is regular and isotropic, only the number of nodes n_x and the corresponding mesh size Δx in the x-direction is mentioned for simplicity. Δ refers to the filter size introduced by the Smagorinsky model with the constant $C_s = 0.1$ when its standard version is used.

When the viscous term is turned on in LES with a coarse resolution (calculations 2 and 16) an interesting phenomenon can be observed. For these "no model LES" free from any extra dissipation, a sub-dissipative behaviour could be expected in view of the underestimation of the viscous term contribution due to the discretization error. Figure 5 clearly shows the opposite trend with a stronger fall of E_k during the transition along with a higher peak of ε_t. A close examination of the time evolution of these two quantities shows that the lack of any explicit SGS model and numerical dissipation is actually slightly sub-dissipative in the early transition by comparison with the three other cases based on $\nu_0 > 0$. This lack of dissipation produces a pile-up of energy near the cutoff wavenumber k_c. This extra energy at small scale overcompensates the essentially subdissipative nature of the numerical operator of the viscous term so that E_k is overdamped as the transition develops further. As seen later in this paper, this overall overdamping is not enough to suppress the spurious energy at small scale. The present overdissipative behaviour obtained using a subdissipative operator is a very simple illustration of the well-known potential contradiction between *a priori* and *a posteriori* analyses of the influence of any subgrid-scale modelling.

When the second derivatives of the Navier-Stokes equations are computed using an over-dissipative scheme with the level of numerical viscosity predicted by the Pao-like solver (calculations 3, 5, 6 and 17–19), the agreement with the DNS is clearly improved as shown in figure 5. The *a priori/a posteriori* paradox is recovered in reverse, namely the extra dissipation is found to slow down the time decrease of E_k during the transition by comparison with the "no model LES" while agreeing remarkably well the DNS data. This agreement suggests that the present targeted numerical dissipation is able to compensate consistently the small-scale dissipation missed by the coarse spatial resolution.

A comparison between the three SVV kernels suggests a slightly better behaviour for the steep SVV kernel at $\nu_0/\nu = 63$ as far as the time evolution of the kinetic energy is concerned (see figure 5). With this particular kernel, no spurious secondary peak on ε_t is observed at $Re = 5000$ while at $Re = 10000$, the first peak of ε_t is more accurately predicted by comparison with DNS. For clarity, only this intermediate case will be used as a reference for the comparison with explicit SGS model, but all the following conclusions are valid for the three SVV kernels.

Figure 6 compares the time evolution of E_k using an implicit (i.e. based on numerical dissipation) or explicit SGS modelling for the two Reynolds num-

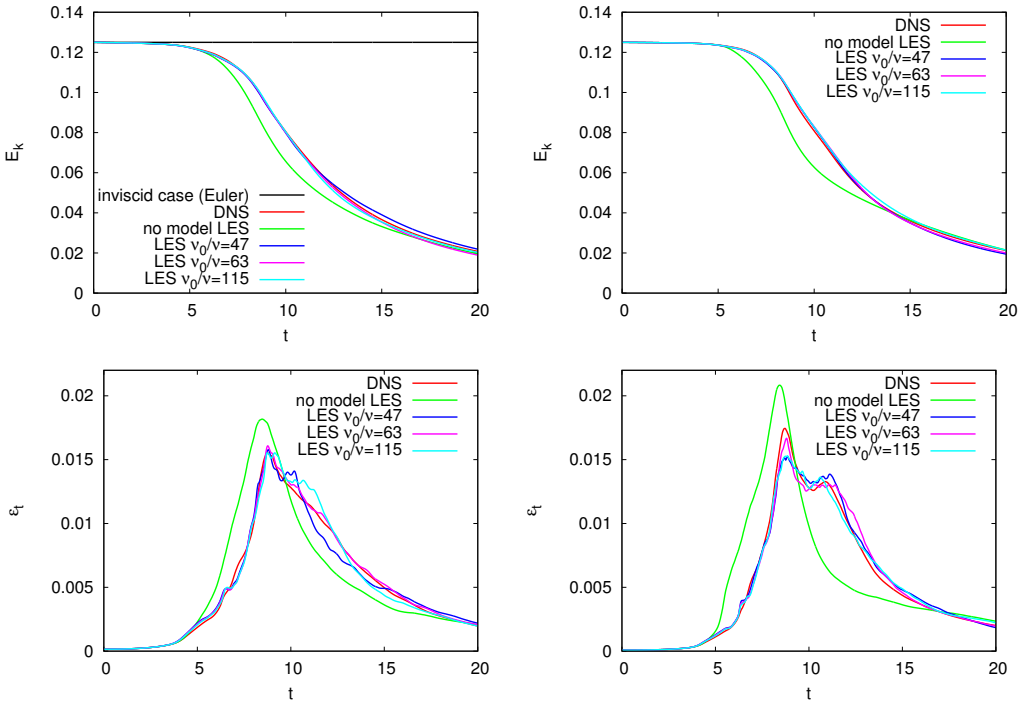

Figure 5: Time evolution of the kinetic energy E_k and its related total dissipation $\varepsilon_t = -dE_k/dt$. Left: $Re = 5000$. Right: $Re = 10000$.

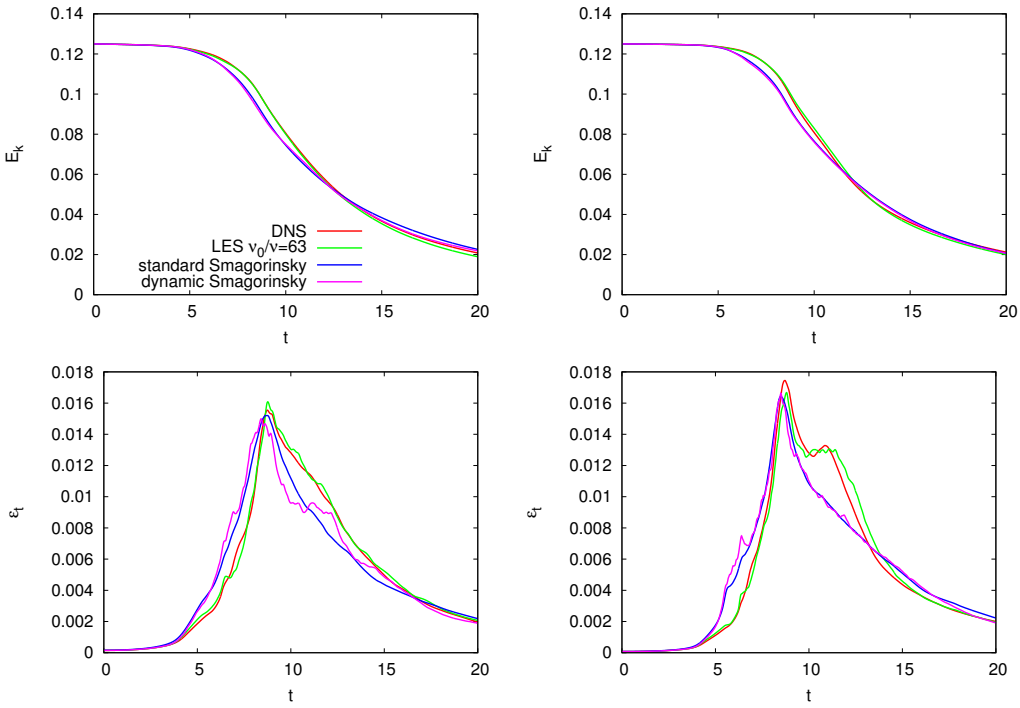

Figure 6: Time evolution of the kinetic energy E_k and its related total dissipation $\varepsilon_t = -dE_k/dt$. Left: $Re = 5000$. Right: $Re = 10000$.

bers considered. Both the standard and dynamic Smagorinsky models are able to improve the results by comparison with the case free of any implicit or explicit SGS modelling (calculations 2 and 16). However, the agreement with DNS is not found as good as when only numerical dissipation is used. In terms of agreement with DNS, the LES based on explicit SGS models can be seen as in between the no model LES and LES based on numerical dissipation. The reason of the deviation from DNS seems to be connected to an overestimation of the total dissipation ε_t during the transition. The use of the dynamic procedure is found to slightly reduce this overdissipative behaviour of the SGS model in the early transition but without any significant impact on the overall agreement with DNS throughout the time evolution of E_k and its related total dissipation ε_t. To highlight the main effects of the implicit and explicit SGS modelling on the computed solutions, a spectral analysis has been performed. The more meaningful results of this analysis are discussed in the next section.

4.3. Kinetic energy spectra

To understand the role played by the artificial viscosity, it is insightful to observe the time evolution of the kinetic energy spectrum $E(k,t)$ [4] For the "no model LES", from the start of the early transition until the end of the calculation, an unrealistic pile-up of energy is clearly observed in the vicinity of the cutoff wavenumber k_c. For this case as for the cases based on an explicit SGS model, this pile-up of energy is maximum just after the turbulent breakdown at $t \approx 10$. Then, thanks to the molecular dissipation combined or not with the SGS model dissipation, this phenomenon is alleviated but still present up to the end of the simulation. To illustrate the resulting shape of the kinetic energy spectra, the intermediate time $t = 14$ is presented in figure 7. This time correspond to the late transition for which the turbulence is fully developed.

The main conclusion provided by the spectra presented in figure 7 is their drastic change in nature depending on the implicit/explicit character of the SGS modelling.

When the present numerical dissipation analogous to high-order SVV is used, $E(k,t)$ strongly falls at large wavenumbers by comparison to DNS. This behaviour is observed throughout the simulation (not shown for conciseness). The spectral range of this strong decrease of $E(k,t)$ with k corresponds essentially to the scales where the artificial dissipation is active as suggested by the SVV kernels presented in figure 2. As expected, the sharper the kernel is, the less this range is extended as clearly shown in figure 7-top. Interestingly, the value of $E(k_c,t)$ is found to be similar for the three SVV kernels, consistently with the Pao-like solver based on criterion (28) that involves the LES kinetic energy spectrum at the cutoff. Note however that this criterion, in terms of relationships between LES and DNS, is not ensured in practice where we have $E_{LES}(k_c,t) \gg E_{DNS}(8k_c,t)$. This discrepancy should probably be associated with the assumptions used to obtain the Pao solution and its numerical counterparts. The residual aliasing errors associated with the discretization, not taken into account in the Pao-like solver, could also be responsible for the higher value of the $E(k_c,t)$ actually observed in the simulations. The signature of these errors can be detected in the slight perturbation of the decay of $E(k,t)$ at $k \approx k_c$ (see figure 7-top). The assump-

[4] Here, even if one dimensional spectra $E(k_x,t)$ are considered, the corresponding quantity is written $E(k,t)$ for simplicity.

tion in the Pao closure that the turbulence is at equilibrium can also explain the discrepancy between the Pao-like model predictions and the LES results. In the present study, the flow is subjected to a complete transition which necessarily deviates from an equilibrium turbulent state. It is worth mentioning that even if the condition $E_{LES}(k_c, t) = E_{DNS}(8k_c, t)$ is not ensured in present calculations, the corresponding error in terms of wavenumber is quite small due to the very steep spectra assumed in the Pao-like model and actually observed in the calculations.

The situation is completely different when an explicit SGS model is used without any extra numerical dissipation. In that case, no strong fall of $E(k, t)$ is observed near the cutoff wavenumber k_c. The opposite behaviour is clearly observed through a reduction of the spectrum slope as k goes to k_c. The slope can even change of sign at $k = k_c$, as a manifestation of a local kinetic energy pile-up that the explicit model is unable to prevent. This feature can be seen in figure 7-bottom even if it is less marked by comparison to earlier times associated with the turbulent breakdown (not shown for conciseness). At $t = 14$, the kinetic energy pile-up at k_c is enough to overestimate locally $E(k, t)$ by comparison with DNS. This anomalous $E(k, t)$ at small scales is present for both Reynolds numbers and both versions (standard and dynamic) of the Smagorinsky model. It is similar, to a lesser degree, to what is obtained when no model (implicit or explicit) is used (see figure 7-top). Also in common with the no model LES, explicit SGS model provides an underestimation of $E(k, t)$ at mid-range wavenumbers compared to DNS and to LES based on numerical dissipation.

One idealised picture in the context of LES is to expect kinetic energy spectra with a constant negative slope near the cutoff wavenumber, this constant corresponding at best to the value $-5/3$ for a Kolmogorov spectrum. In the present results, this picture corresponds better to what is obtained using an explicit SGS model, the use of numerical dissipation providing very steep spectra in a significantly extended range of scales. The shape of the LES spectrum is in fact directly connected to the filter invoked to separate large from small scales. However, because in a conventional Smagorinsky model this filter is only introduced by the model itself, it is difficult to have a clear idea about the reliability of any given LES spectrum. This point is addressed in sections 4.5 and 4.7 through a numerical convergence study followed by an estimation of the filtering effect of the two types (explicit or implicit) of SGS modelling. Before these two last steps, a brief investigation of instantaneous fields is proposed in the next section in order to connect the

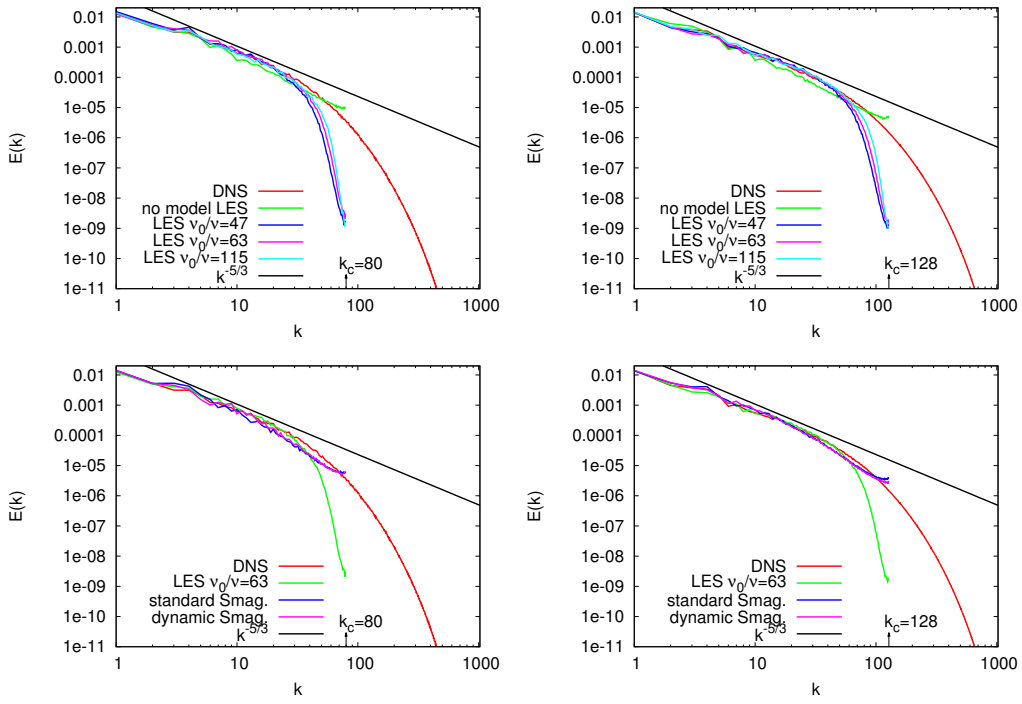

Figure 7: Kinetic energy spectra $E(k,t)$ at $t = 14$. Left: $Re = 5000$. Right: $Re = 10000$.

spectral modifications of the solution to changes in the vortical structures of the flow.

4.4. Instantaneous visualisation

Visualizations based on Q-criterion show the development of unrealistic vortical structures subjected to a background noise for the no model case but also for the LES based on explicit SGS models (see figure 8). The corresponding production of small-scale spurious oscillations is found to distort significantly the large-scale vortices by comparison with DNS in the sense that the vortical pattern obtained cannot be viewed as a filtered state of the DNS solution. Conversely, the use of a calibrated numerical viscosity in the LES SVV-like and steep SVV $\nu_0/\nu = 47, 63$ cases allows the formation of smooth structures free of spurious small-scale perturbations. The visualisations obtained using this level of numerical dissipation correspond clearly more to what is expected from LES through the development of smooth vor-

tices that can be viewed as spatially filtered by comparison with their DNS counterparts.

The present comparative comments about the instantaneous fields relate to any time of the calculations subsequent to the turbulence transition. The difference between LES based on implicit or explicit SGS modelling is more marked slightly after the total dissipation peak, i.e. when the turbulent breakdown is the most active. The visualisations presented in figure 8 are an illustration of the difference in nature of the results from the two types of LES discussed in this study. This difference is persistent after the transition crisis when fully turbulent conditions are established, as at the time $t = 14$ presented in figure 8. This means that the present conclusions are not limited to the transitional state. The two explicit SGS models are unable to deal correctly with well-established turbulence, although it corresponds to the framework they are designed for. On the contrary, the use of numerical dissipation enables better predictions of the kinetic energy in terms of time evolution and level at mid-range wavenumbers. In addition, the coherence of vortices seems to be better preserved throughout the calculation. The LES based on numerical dissipation exhibit the regularity features expected in the context of LES where only large-scale motions should be captured while minimizing the impact of small-scales not correctly taken into account by the computational mesh. This qualitative distinction between large- and small-scale contributions is less clear in LES based on the explicit SGS models. For the present flow, no significant improvement is provided by the dynamic version of the Smagorinsky model and the loss of regularity is observed at the two Reynolds number considered.

Following the procedure of [67], the effective viscosity has been estimated for the LES carried out. The values obtained are similar for the LES based on implicit and explicit SGS modelling. For instance, at $Re = 10000$ and $t = 14$, the resulting effective Reynolds number based on the Taylor microscale is $Re_{\lambda_{\text{eff}}} \approx 135$ for the LES by comparison to the reference DNS value $Re_\lambda \approx 200$. For the same spatial resolution and flow configuration, [67] have reported significantly lower effective $Re_{\lambda_{\text{eff}}} \approx [38 - 52]$ obtained by implicit LES based on the solving of the Euler equations (nominally inviscid flow). The present value $Re_{\lambda_{\text{eff}}} \approx 135$ suggests that the artificial viscous effects are less invasive in the present type of controlled implicit LES. In physical terms, this behaviour enables the computed flow by LES to exceed the mixing-layer threshold corresponding to $Re_\lambda \approx 100$.

At this stage, nothing can be concluded about the role of numerical errors

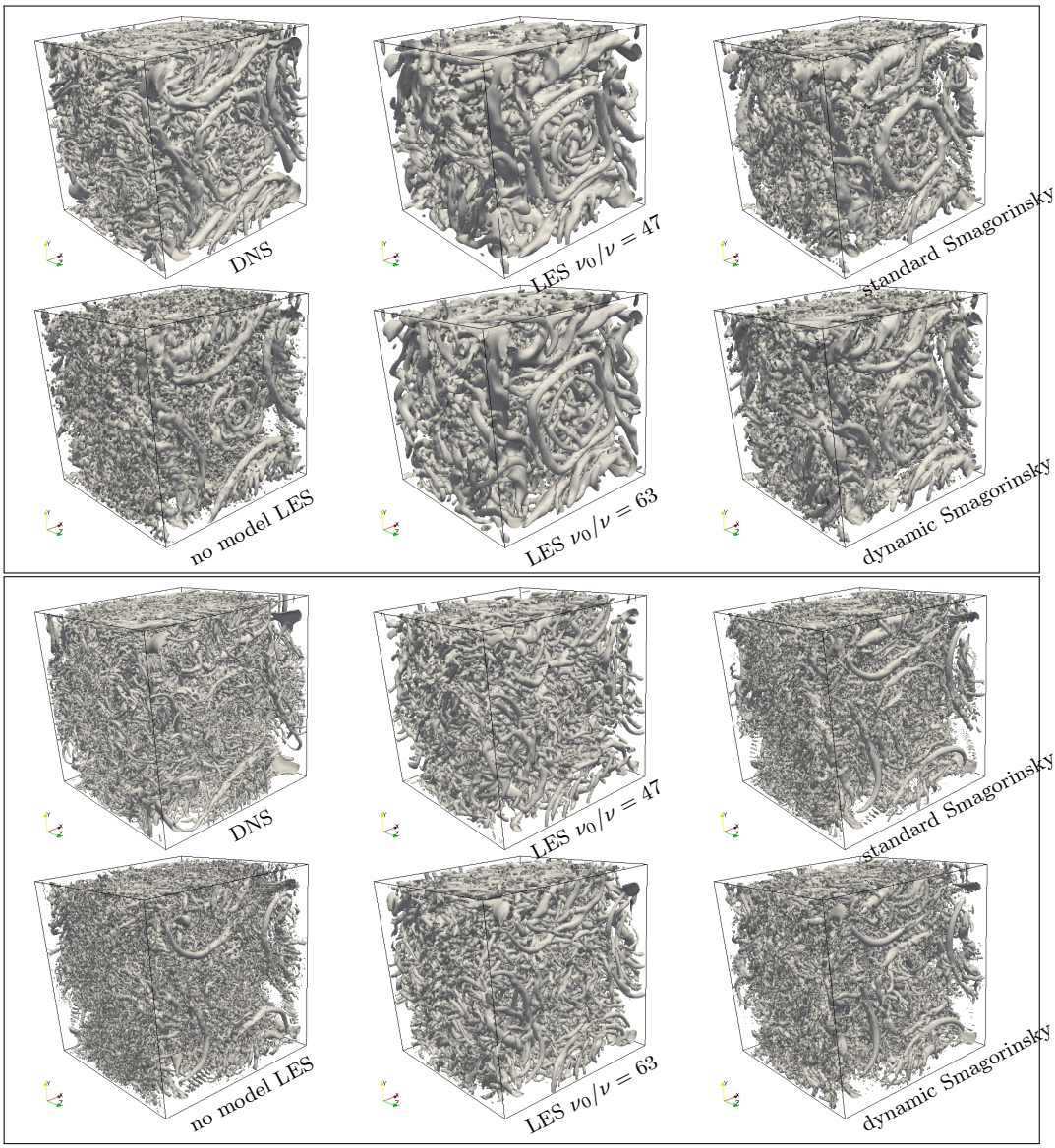

Figure 8: Isosurface of Q-criterion. Top: $Re = 5000$ ($Q = 1$). Bottom: $Re = 10000$ ($Q = 4$).

in the lower performance of standard and dynamic Smagorinsky models. This crucial point is addressed in the next section through an analysis where the contribution of the discretization is gradually reduced up to a point where it becomes negligible.

4.5. Numerical convergence using Smagorinsky model at $Re = 5000$

In LES, the notion of convergence can refer to two different approaches that should be clearly distinguished before going further in the analysis.

First, the convergence can be related to the SGS model behaviour as its filtering effect is reduced. Explicit LES models introduce a filter size Δ. In this case, the SGS model convergence refers to its behaviour as $\Delta \to 0$. This concept is free from any consideration about the discretization of LES equations when based on continuous equations as for the Smagorinsky model. In this framework, the property expected is that the LES solution converges toward the solution of the Navier-Stokes equations (potentially provided by DNS) when $\Delta \to 0$.

In this study, we address only the second type of convergence which concerns the influence of an increase of spatial resolution (i.e. $\Delta x \to 0$) while keeping constant the filter length Δ. This type of convergence is purely numerical because all the physical and modelling parameters can be kept constant while reducing the numerical error as $\Delta x \to 0$. It should be stressed that because the code Incompact3d is a sixth-order accurate solver, the resulting convergence rate is very high compared to most codes used in CFD. As a consequence, the criticisms which follow should be viewed as euphemistic in the context of the most popular practice of LES.

Here, we present series of four calculations obtained at $\Delta/\Delta x = 1, 2, 3, 4$ while keeping constant the filter length Δ (see table 1 for details). Thanks to the sixth-order accuracy, the corresponding reduction of errors is equal to $4^6 = 4096$ as Δx goes from Δ to $\Delta/4$. This type of numerical convergence is very easy to carry out using the standard Smagorinsky model (3) as it is only composed of the constant C_s, the filter length Δ and spatial derivatives.

For the dynamic Smagorinsky, the numerical convergence is technically more delicate to obtain due to the test filter that is typically a discrete operator primary connected to the computational mesh Δx and not to the filter length Δ. The discrete compact sixth-order filter used in this study has this feature of scaling on Δx rather on Δ. To overcome this technical difficulty, series of three calculations using $\Delta > \Delta x$ have been performed by carrying out the test filtering in the Fourier space using the exact transfer

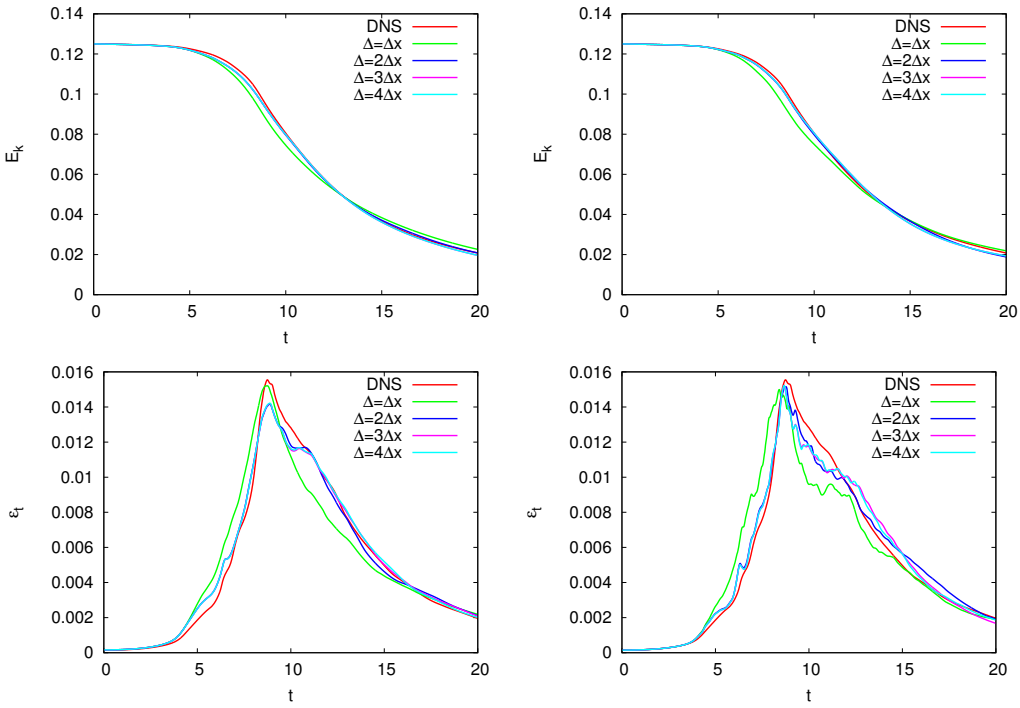

Figure 9: Time evolution of the kinetic energy E_k and its related total dissipation $\varepsilon_t = -dE_k/dt$. Left: standard Smagorinsky. Right: dynamic Smagorinsky.

function $T_f(k)$ scaled on Δ while extending its kernel as $T_f(k) = 0$ for $k_\Delta < k < k_c$ as illustrated in figure 10-left. This treatment in Fourier space is possible thanks to the periodicity in the three directions of space. In this way, the numerical convergence can be ensured by keeping all the parameters constant except the mesh size Δx.

The time evolution of the kinetic energy is presented in figure 9 for the two series of four calculations based on the standard and dynamic Smagorinsky models. As the numerical errors are reduced, a significant improvement of the agreement with DNS can be observed for the two versions of the explicit SGS model. The main improvement is obtained through a mesh refinement by a factor 2 that corresponds in itself to a reduction of $2^6 = 64$ of the numerical errors. This first observation emphasizes the major importance of the discretization in the actual performance of an explicit SGS model.

In figure 9, the convergence of the dynamic Smagorinsky model could be considered as slightly slower when examined after the turbulence transition.

However, this conclusion should not be overstated due to the loss of predictability of the flow after the turbulent breakdown. Very small differences introduced at small scales by the discretization and SGS model are amplified by the non-linear dynamics while propagating to the large scales through an error backscatter process. For a review about the concept of inverse cascade of unpredictability, the reader is referred to [39]. Here, the spatially averaged quantities being only based on a single flow realization, the loss of predictability after the turbulent transition does not allow an exact comparison of statistics obtained from the various LES and DNS. Because the inverse cascade of error contaminates gradually larger and larger scales, the time evolution of the kinetic energy is eventually impacted up to the smallest wavenumbers that are the most energy containing while being poorly converged statistically. This process introduces a significant uncertainty in the prediction of the final evolution of the flow for which the present LES cannot be deterministic. In other words, the residual differences observed at $t \gtrsim 10$ should not be considered as a lack of numerical convergence but as the signature of loss of predictability.

To confirm the numerical convergence of the dynamic procedure, the time evolution of the constant $C_s(t)$ estimated by (5) is plotted in figure 10 for the four mesh resolutions at $Re = 5000$. The estimation of $C_s(t)$ is found to be highly sensitive to the numerical errors while enabling a numerical convergence as they are reduced. When the turbulence become fully established after the dissipation peak, the dynamic procedure provides the estimation $C_s \approx 0.1$. For consistency purposes, this value has been chosen when the standard Smagorinsky is used.

The numerical convergence can also be noticed by comparing the kinetic energy spectra obtained at different spatial resolutions as exhibited in figure 11. The main lesson from this comparison is that the spectrum obtained when $\Delta = \Delta x$ is strongly distorted by numerical errors. The contaminated spectral range is wide with a significant underestimation of $E(k,t)$ for $0.1k_\Delta \lesssim k \lesssim 0.75k_\Delta$ followed by a strong overestimation at higher wavenumbers $0.75k_\Delta \lesssim k < k_\Delta$. This numerical convergence analysis enables the conclusion that this distortion previously observed by comparison with DNS is not a feature of the Smagorinsky model but the consequence of discretization errors.

Another important conclusion is that the SGS dissipation introduced by the use of an eddy viscosity does not produce a strong fall of $E(k,t)$ for $k > k_\Delta$ even when numerical errors become negligible. The decrease of the kinetic energy spectrum for converged LES based on Smagorinsky model is

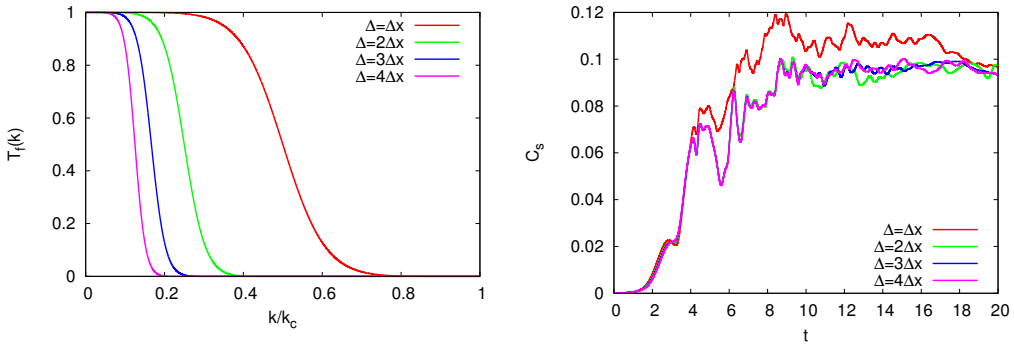

Figure 10: Left: test filters $T_f(k)$ as used to ensure the scaling on Δ. Right: Time evolution of Smagorinsky constant $C_s(t)$ as predicted by the dynamic procedure.

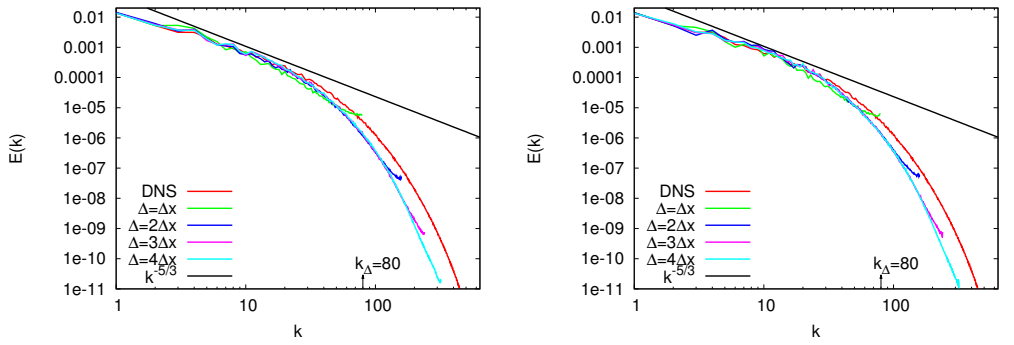

Figure 11: Kinetic energy spectra $E(k,t)$ at $t = 14$. Left: standard Smagorinsky. Right: dynamic Smagorinsky.

qualitatively similar to its DNS counterpart, suggesting a moderate filtering effect. This point is discussed further in the next section. Because of the slow decrease of $E(k,t)$, a requirement resolution based on the truncation error would make the approach potentially very demanding in terms of computational resources. This is a major difference with the approach based on numerical dissipation that enables the drastic reduction of the truncation error through a strong fall of $E(k,t)$. For instance, it is worth mentioning that using the standard or dynamic Smagorinsky models, the spatial resolution must be almost tripled in each direction, increasing then by a factor about 80 the computational cost, in order to have the same value of the kinetic energy at the cutoff wavenumber $E(k_c) \approx 10^{-9}$. This ability of present high-order numerical dissipation to efficiently damp small-scale energy is probably its major asset.

As a last illustration of the consequences of numerical errors using Smagorinsky model, figure 12 presents instantaneous visualisations of Q-criterion at $t = 14$ using the normal mesh resolution ($\Delta = \Delta x$) and the one refined twice ($\Delta = 2\Delta x$). The spurious oscillations are found to be gradually removed as the spatial resolution is increased while restoring the realism of the flow vortices. The presence of "wiggles" with $\Delta = \Delta x$ is a clear indication that the physical scales allowed by the Smagorinsky model are significantly smaller than the one allowed by the mesh.

4.6. Numerical convergence using numerical dissipation at $Re = 5000$

A criticism frequently levelled at implicit LES is that the modelling contribution cannot be distinguished from the numerical errors, both being intricately linked. This link would make impossible to analyse the numerical convergence in the sense addressed in the previous section. In fact, this impossibility is not conceptual but technical. For instance, because the present numerical dissipation can be written as a spectral viscosity with a clearly defined kernel, a numerical convergence study can be carried out. Even if this extra dissipation is essentially an error, it can be interpreted as a model while keeping it constant (independent of the computational mesh) as the spatial resolution is increased. This procedure was followed to examine the sensitivity of the present controlled implicit LES on the numerical errors. Technically, the principle is the same as for the test filter in the previous section thanks to the periodicity that enables the application of any SVV kernel (as those illustrated in figure 2) in the Fourier space during the simulation. The SVV kernel is scaled on k_Δ instead of k_c while being extended

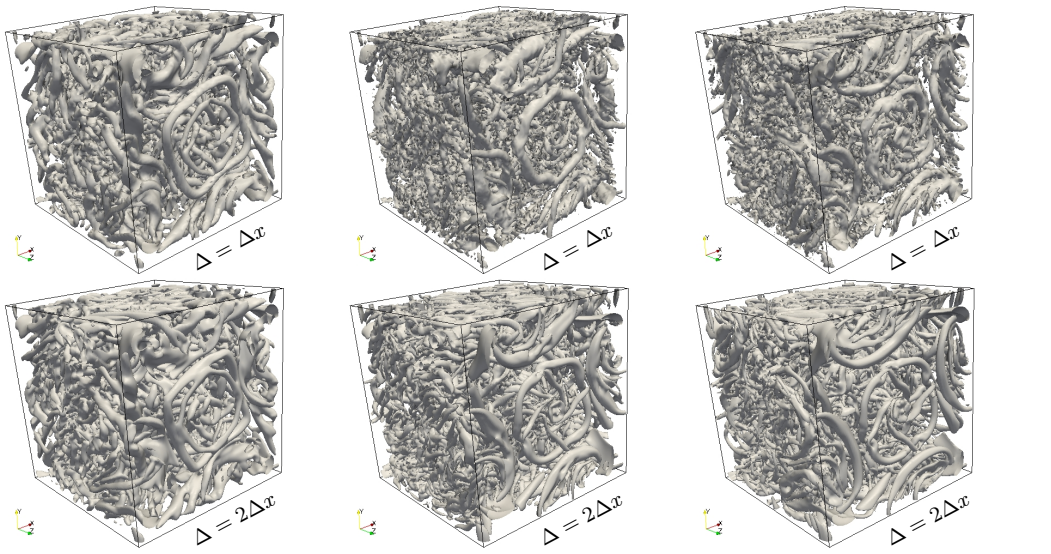

Figure 12: Isosurface of Q-criterion ($Q = 1$). Top: LES at normal mesh resolution ($\Delta = \Delta x$). Bottom: LES at refined mesh resolution ($\Delta = 2\Delta x$).

as $\nu''(k)/\nu_0 = 1$ for $k_\Delta < k \leq k_c$ (as illustrated in figure 13-top). Then, the mesh size Δx can be chosen smaller that the reference length Δ in order to perform a numerical convergence analysis of the implicit model.

Time evolution of the total dissipation ε_t and kinetic spectra at $t = 14$ are compared in figure (13) for the normal ($\Delta = \Delta x$) and refined ($\Delta = 2\Delta x$) LES based on the steep SVV with $\nu_0/\nu = 63$. Except the unavoidable slight differences due to the inverse cascade of unpredictability after the flow transition [39], both results are found in excellent agreement. This quite formal validation means that the dominant dissipative numerical errors make the results insensitive to the other sources of numerical errors. It can be concluded that the condition $\Delta = \Delta x$ is able to provide numerically well converged solutions with a small truncation error. Numerical dissipation is the main source of numerical error that is diverted in order to work as an implicit SGS model while dominating the other sources of numerical errors. This very low sensitivity to extra numerical errors makes the approach robust and efficient in the sense that no extra refinement is required for a given SVV kernel.

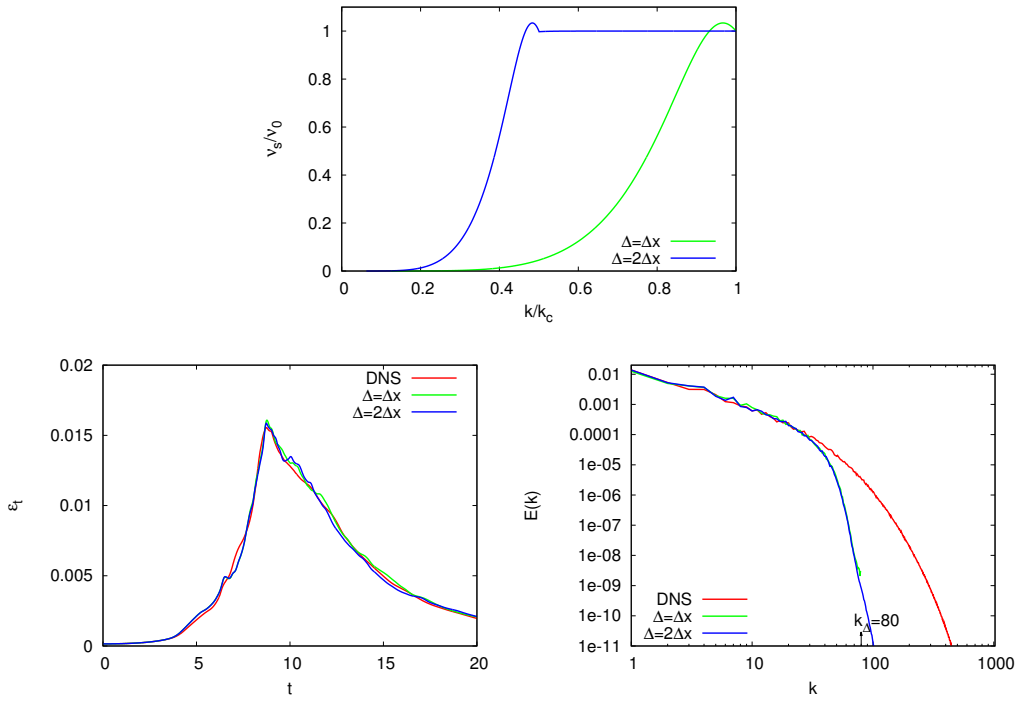

Figure 13: Data from LES using steep SVV with $\nu_0/\nu = 63$ at two different spatial resolutions. Top: conventional kernel for $\Delta = \Delta x$ and extended kernel for $\Delta = 2\Delta x$. Bottom-left: time evolution of the total dissipation ε_t. Bottom-right: kinetic energy spectra $E(k,t)$ at $t = 14$.

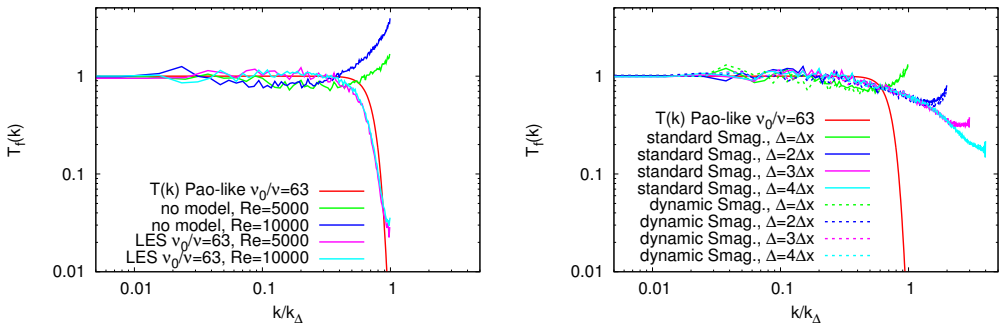

Figure 14: Transfer functions $T_f(k,t)$ associated with the filtering effect of the implicit and explicit SGS models. Examples at $t = 14$. Figure right corresponds to results obtained at $Re = 5000$ for the numerical convergence study.

4.7. Estimation of the filtering effect

Before providing the main conclusions of the study, it can be enlightening to examine the filtering effect associated with the application of the numerical dissipation or to the explicit SGS model. The transfer function corresponding to the filtering effect can be estimated as

$$T_f(k,t) = \sqrt{\frac{E_{LES}(k,t)}{E_{DNS}(k,t)}}. \tag{35}$$

The spectra $E_{LES}(k,t)$ and $E_{DNS}(k,t)$ can correspond to the DNS and LES data, but also to the Pao (DNS) and Pao-like (LES) spectra in order to estimate *a priori* the filtering effect of one given SVV kernel for a particular value of ν_0/ν. Examples of these transfer functions are presented in figure 14-left at the particular time $t = 14$ already chosen for the spectra and visualisations presented in figures 7, 11 and 8.

The examination of transfer functions in figure 14-left shows clearly the good behaviour of present high-order SVV that enables the damping of the kinetic energy at small scales. The improvement obtained through this damping is obvious by comparison with the no model cases where the transfer functions are completely inappropriate with a strong "defiltering" effect at small scales (worsened at $Re = 10000$) and a filtering at small wavenumbers that is against the LES goal to capture accurately the large-scale dynamics by checking the condition $T_f(k) \approx 1$.

The agreement between $T_f(k)$ obtained by LES and predicted through the Pao-like closure on the basis of high-order SVV is mainly qualitative. For instance, the condition $T_f(k) \approx 1$ is ensured up to $k \approx 0.5k_c$ for the LES against $k \approx 0.7k_c$ for the Pao-like closure (see figure 14-left). At the cutoff wavenumber, as previously noticed directly on the spectra, the value of $T_f(k_c)$ is clearly higher in LES in comparison with the Pao-like solver. To summarize, the effect of SVV in actual LES is found to be more active in the mid-range wavenumbers and less active near the cutoff wavenumber. Despite this discrepancy, the high-order numerical dissipation actually ensures a consistent filtering effect with a strong attenuation of the kinetic energy by comparison with DNS, this feature enabling a significant reduction of the truncation error. An interesting feature is the excellent collapse between the transfer functions obtained by the two equivalent LES performed at different Reynolds numbers. This collapse, clearly shown in figure 14-left, suggests a certain robustness of the approach that is able to mimic the universal behaviour assumed in the Pao closure. Moreover, no local bump of $T_f(k)$ before its fall can be detected, suggesting that no significant bottleneck effect [87] is introduced by the increase of the spectral viscosity near the cutoff wavenumber k_c.

The transfer functions obtained with the standard and dynamic Smagorinsky models are particularly helpful to understand the intrinsic limitation of these explicit SGS models. First, the figure 14-right clearly shows that the option $\Delta = \Delta x$, almost systematically used in practical LES, produces a very unrealistic transfer function with a strong defiltering effect in the spectral range $0.6k_\Delta \lesssim k < k_\Delta$ and a significant filtering effect in the range $0.2k_\Delta \lesssim k < 0.6k_\Delta$. This practical filtering is clearly in contradiction with the filtering invoked in the LES formalism. When a damping of kinetic energy is expected at small scales, amplification is obtained, and when a minor influence is expected at large scales, a significant damping is observed. This anomaly is rectified when a finer mesh is used, confirming that the numerical errors are the main responsible for it. However, even when numerical errors become negligible as for the case $\Delta = 4\Delta x$, the k-decrease of the transfer function is found to be surprisingly weak. The filtering effect associated with the Smagorinsky model is found to be particularly soft. This feature can be seen as a strong weakness of the Smagorinsky model in terms of ability to reduce the number of degrees of freedom of the problem, this reduction being the ultimate goal of the LES approach.

5. Discussion and conclusion

This study is an attempt to compare, and to some extent combine, two antagonistic LES approaches. The first approach is based on the use of artificial dissipation, as a numerical error, to ensure the regularity of the solution. It has no well-defined formalism with *a priori* a lack of clear physical scaling. Its action is implicit in the sense that it is only embedded in the numerical method without any modification of the governing equations to discretize. The second approach is based on explicit SGS modelling guided by a formalism based on modified governing equations and physical arguments to scale the model. It does not integrate the notion of numerical error in the modelling itself.

As a generic example of what can be done with these two approaches, the academic Taylor-Green vortex problem is computed using a high-order flow solver which is kinetic energy conserving in the discrete sense in the inviscid limit (up to the accuracy of the time advancement). As an explicit SGS model, the very popular Smagorinsky model has been assessed by considering its standard and dynamic versions. It is found that even if this model improves results by comparison to the lack of any explicit or implicit model, it cannot challenge the simple use of numerical dissipation. The slight improvement offered by the dynamic procedure does not change this conclusion. The main reason of the poor performance of the Smagorinsky model is found to be related to its sensitivity to numerical errors. The role of numerical errors has been unambiguously shown in this work through a numerical convergence analysis of the solution. In its normal use where the filter length Δ is equal to the mesh size Δx, the Smagorinsky model is found to be unable to control the development of small-scale oscillations. The production of spurious oscillations can be seen as a partial thermalization [88] of the turbulent flow that distorts strongly its kinetic energy spectrum not only at high wavenumbers (where a pile-up of energy is observed) but also in the mid-range wavenumbers. This contamination of lower wavenumbers is assumed to be the consequence of triad interactions between the unrealistic thermalized zone at high wavenumber and the rest of the spectrum.

When the numerical errors are made negligible through the use of a mesh size Δx significantly smaller than filter length Δ, the production of spurious small-scale oscillations can be avoided with the Smagorinsky model, but the corresponding computational cost makes the approach inefficient. Basically, the numerical convergence analysis shows that the filtering effect associated

with the Smagorinsky model is very soft. As a consequence, this model is unable to provide a significant reduction of the number of degrees of freedom, with or without the dynamic procedure. In other words, to perform LES using the Smagorinsky model while ensuring a minor role of numerical errors, the spatial resolution requirement is only marginally reduced by comparison with DNS. This is obviously a strong limitation of the model.

On the contrary, when high-order numerical dissipation is used, the production of small-scale oscillations can be efficiently controlled. In this study, an original method to provide targeted numerical dissipation is presented. This artificial dissipation is introduced via the discretization of the viscous term and can be seen as spectral vanishing viscosity that can be easily shaped in order to control its value at the cutoff wavenumber as well as its spectral distribution. Using this favourable feature, a simple method to scale the level of spectral viscosity has been proposed. This method is based on a very simple closure of the Lin equation taking the numerical dissipation into account. The resulting Pao-like spectrum solutions are used to scale appropriately the spectral viscosity on a physical basis. The scaling is based on the idea that ideally, the truncation error of the LES should be similar to the truncation error of its hypothetical DNS counterpart which would be performed at a significantly higher spatial resolution.

The LES with the values obtained from the physical scaling of the numerical dissipation are found to be in better agreement with DNS than the LES with a Smagorinsky model. The spectral analysis shows a strong reduction of the kinetic energy near the cutoff wavenumber as expected. This ability to ensure the smoothness of the solution is found to improve the realism of the vortical structures. In addition, the lack of any thermalization near the cutoff wavenumber is found to significantly improve the kinetic energy spectrum in the mid-range wavenumbers. It is as if the "sacrifice" of small-scale fluctuations, not well resolved by the mesh and then strongly damped by the artificial dissipation, was eventually beneficial for the prediction of large-scale motions. Schematically, the artificial damping of the second half of the Fourier modes improves the prediction of their first half. Without this artificial damping, as for the Smagorinsky model with $\Delta = \Delta x$, the range of large scales correctly predicted is reduced by more than half while producing unrealistic vortical structures.

When high-order numerical dissipation is used, the transfer function associated with the filtering effect is found to be attractive in its ability to reduce the number of degrees of freedom of the problem. This is a major advantage

of the method directly connected to the calibration technique in order to ensure a low truncation error. This property makes the method insensitive to an increase of the spatial resolution. In that sense, if the extra dissipation is interpreted as spectral viscosity, the results can be considered as numerically converged and weakly sensitive to extra numerical errors provided that high-order schemes with good spectral properties are used. This is a fundamental difference from the Smagorinsky model which is highly sensitive to numerical errors.

An important conclusion of this study is that it is highly beneficial for LES based on high-order schemes to ensure the smoothness of the solution through an artificial damping of scales of wavelength less than four meshes (of wavenumbers $k_c/2 < k < k_c$). This damping seems to be enough to enable the LES to provide accurate results without any extra explicit modelling.

Contrary to the most widespread implicit LES where the numerical dissipation is applied through the convective term, the present strategy where both physical and numerical dissipations are exclusively ensured by the viscous term is found to offer flexibility with a convenient basis to combine numerics and physics through a relevant calibration. However, it should be recognized that a rigorous formalism is still missing in the sense that the type of solution is not clearly defined. Conceptually, the approach consists in solving a problem with a reduced number of degrees of freedom. The simple Pao-like model allows an *a priori* estimation of the filtering operator associated with this reduction but only in an academic situation essentially based on homogenous and isotropic features of both turbulence (at small-scales) and computational mesh. In the present calculations, the *a posteriori* computation of the filtering effect is in reasonable agreement with its *a priori* estimation but it would be difficult to carry out a similar study for a less academic flow with for instance the strong inhomogeneity and anisotropy observed in wall turbulence.

It does not mean that the present regularisation technique cannot work for inhomogenous and anisotropic turbulence, as suggested by the successful results briefly reported in [75] for a turbulent channel and also as supported by the more extensive study [44] for a turbulent jet impinging on a heated wall. An interesting conclusion of these studies is that no near-wall correction was required to obtain reliable turbulent statistics. This behaviour corresponds to one of the most attractive features of implicit LES. Naturally, more validations are certainly required for a wide spectrum of turbulent flows in order to confirm the reliability of the present approach. The return to a

more academic situation was the initial motivation of this work in order to better understand the nature of the implicit modelling while finding a pragmatic way to calibrate physically the corresponding numerical viscosity.

As a very general recommendation for the treatment of inhomogenous and anisotropic turbulent flow configuration, including near-wall turbulence, we suggest to design first the mesh that the hypothetical DNS would require and then coarsen the mesh to obtain the LES mesh by a constant ratio everywhere in the computational domain and in the three directions of space. This ratio is the only input required by the Pao-like model to provide an estimation of the level of numerical viscosity to be introduced in the LES.

A last remark should be made concerning the use of vanishing spectral viscosity. When LES is examined in the spectral space with a scale separation through a cutoff filter, two-point closure theory suggests that the spectral viscosity has a plateau-cusp profile [37, 38, 39]. The cusp feature is reproduced by the present approach and the successful results suggest that it is an important feature to capture. However, the vanishing behaviour means that the plateau value is zero. The lack of any modelling of the direct influence of the filtered small-scales on the dynamics at large scale is in contradiction with previous studies based on two-point closures [39], but the current work was carried out for relatively small values of $\pi k_\eta/k_c$ (only an order of magnitude or less) for which the lack of such modelling can indeed be expected not to matter. The assumption that large-scale dynamics is almost inviscid at high-Reynolds numbers without "feeling" the small-scale fluctuations is probably a weakness of any approach based on vanishing spectral viscosity if higher values of $\pi k_\eta/k_c$ are to be tried. For the Reynolds numbers considered in this study, the vanishing feature allows successful results with our relatively small values of $\pi k_\eta/k_c$, but for higher Reynolds numbers where the ratio $\pi k_\eta/k_c$ would have to be increased by necessity, let alone by choice, a modelling of distant interactions will most probably be required. An extra complication is that the now known non-Kolmogorov, i.e. non-stationary, cascade dynamics of much of the inertial range [85] will need to be taken into account and will modify existing models of distant interactions as well as the Pao-like approach used here. To address these points, non-vanishing spectral viscosities as in the spectral subgrid-scale model of [38] will need to be considered and adapted or modified so that higher Reynolds numbers may be realistically reached.

Acknowledgement

This work was granted access to the HPC resources of TGCC under the allocation 2014/2015-2a0912 made by GENCI.

[1] B. Geurts, Elements of direct and large-eddy simulation, Edwards, 2004.

[2] P. Sagaut, Large eddy simulation of incompressible flow: an introduction, 2nd Edition, Springer-Verlag, 2005.

[3] M. Lesieur, O. Métais, P. Comte, Large-eddy simulation of turbulence, Cambridge University Press, 2005.

[4] S. Ghosal, P. Moin, The basic equations for the large eddy simulation of turbulent flows in complex geometry, J. Comp. Phys. 118 (1995) 24–37.

[5] S. Ghosal, An analysis of numerical errors in large-eddy simulations of turbulence, J. Comp. Phys. 125 (1996) 187–206.

[6] P. Moin, K. Mahesh, Direct numerical simulation: a tool in turbulence research, Ann. Rev. Fluid Mech. 30 (1998) 539–578.

[7] F. K. Chow, P. Moin, A further study of numerical errors in large-eddy simulations, J. Comp. Phys. 184 (2003) 366–380.

[8] B. J. Geurts, F. van der Bos, Numerically induced high-pass dynamics in large-eddy simulation, Phys. Fluids 125103 (2005) 1–12.

[9] J. Berland, C. Bogey, C. Bailly, A study of differentiation errors in large-eddy simulations based on the EDQNM theory, J. Comp. Phys. 227 (2008) 8314–8340.

[10] N. Park, K. Mahesh, Analysis of numerical errors in large eddy simulation using statistical closure theory, J. Comp. Phys. 222 (2007) 194–216.

[11] A. W. Vreman, N. D. Sandham, K. H. Luo, Compressible mixing layer growth rate and turbulence characteristics, J. Fluid Mech. 320 (1996) 235–258.

[12] J. Meyers, B. J. Geurts, M. Baelmans, Database analysis of errors in large-eddy simulation, Phys. Fluids 15 (9) (2003) 2740–2755.

[13] J. Meyers, B. J. Geurts, M. Baelmans, Optimality of the dynamic procedure for large-eddy simulation, Phys. Fluids 045108 (2005) 1–9.

[14] J. Meyers, B. J. Geurts, P. Sagaut, A computational error-assessment of central finite-volume discretizations in large-eddy simulation using a smagorinsky model, J. Comp. Phys. 227 (2007) 156–173.

[15] O. L. Maître, O. M. Knio, Spectral Methods for Uncertainty Quantification, Springer, 2010.

[16] H. N. Najm, Uncertainty quantification and polynomial chaos techniques in computational fluid dynamics, Ann. Rev. Fluid Mech. 41 (2009) 35–52.

[17] J. Boris, F. Grinstein, E. Oran, R. Kolbe, New insights into large-eddy simulation, Fluid Dynamics Research 10 (1992) 199–228.

[18] C. Fureby, F. F. Grinstein, Large eddy simulation of high-Reynolds-number free and wall-bounded flows, J. Comp. Phys. 181 (1) (2002) 68–97.

[19] L. G. Margolin, W. J. Rider, F. F. Grinstein, Modeling turbulent flow with implicit LES, J. Turbulence 7 (15) (2006) 1–28.

[20] B. Thornber, A. Mosedale, D. Drikakis, On the implicit large eddy simulations of homogeneous decaying turbulence, J. Comp. Phys. 226 (2007) 1902–1929.

[21] D. Drikakis, M. Hahn, A. Mosedale, B. Thornber, Large eddy simulation using high-resolution and high-order methods, Philosophical Transactions of the Royal Society of London A: Mathematical, Physical and Engineering Sciences 367 (1899) (2009) 2985–2997.

[22] I. W. Kokkinakis, D. Drikakis, Implicit large eddy simulation of weakly-compressible turbulent channel flow, Computer Methods in Applied Mechanics and Engineering 287 (2015) 229–261.

[23] A. Jameson, W. Schmidt, E. Turkel, Numerical solution of the Euler equations by finite volume methods using Runge-Kutta time-stepping schemes, AIAA paper 1981-1259.

[24] C. K. W. Tam, J. C. Webb, Z. Dong, A study of the short wave components in computational acoustics, J. Comput. Acous. 1 (1) (1993) 1–30.

[25] C. Bogey, C. Bailly, Large eddy simulations of transitional round jets: influence of the Reynolds number on flow development and energy dissipation, Phys. Fluids 18 (6) (2006) 1–14.

[26] C. Bogey, C. Bailly, Computation of a high Reynolds number jet and its radiated noise using large eddy simulation based on explicit filtering, Computers and Fluids 35 (2006) 1344–1358.

[27] C. Bogey, C. Bailly, Turbulence and energy budget in a self-preserving round jet: direct evaluation using large eddy simulation, J. Fluid Mech. 627 (2009) 129–160.

[28] J. Berland, P. Lafon, F. Daude, F. Crouzet, C. Bogey, C. Bailly, Filter shape dependence and effective scale separation in large-eddy simulations based on relaxation filtering, Computers and Fluids 47 (2014) 65–74.

[29] G. Aubard, P. S. Volpiani, X. Gloerfelt, J.-C. Robinet, Comparison of subgrid-scale viscosity models and selective filtering strategy for large-eddy simulations, Flow Turb. Combust. 91 (3) (2013) 497–518.

[30] J. Mathew, R. Lechner, H. Foysi, J. Sesterhenn, R. Friedrich, An explicit filtering method for large eddy simulation of compressible flows, Phys. Fluids 15 (8) (2003) 2279–2289.

[31] P. Schlatter, S. Stolz, L. Kleiser, Analysis of the SGS energy budget for deconvolution- and relaxation-based models in channel flow, in: E. Lamballais, R. Friedrich, B. J. Geurts, O. Métais (Eds.), Direct and large-eddy simulation VI, ERCOFTAC series, Springer, 2006, pp. 135–142.

[32] J. A. Domaradzki, N. A. Adams, Direct modelling of subgrid scales of turbulence in large eddy simulations, J. Turbulence 3 (2002) N24.

[33] S. Hickel, N. A. Adams, J. A. Domaradzki, An adaptive local deconvolution method for implicit LES, J. Comp. Phys. 213 (1) (2006) 413–436.

[34] S. Hickel, N. A. Adams, On implicit subgrid-scale modeling in wall bounded flows, Phys. Fluids 19 (10) (2007) 1–13.

[35] J. A. Domaradzki, Large eddy simulations without explicit eddy viscosity models, Int. J. Comp. Fluid Dynamics 24 (10) (2010) 435–447.

[36] F. F. Grinstein, L. G. Margolin, W. J. Rider (Eds.), Implicit Large Eddy Simulation: Computing Turbulent Fluid Dynamics, Cambridge Univ. Press., 2007.

[37] R. H. Kraichnan, Eddy viscosity in two and three dimensions, J. Atmos. Sci. 33 (1976) 1521–1536.

[38] J. P. Chollet, M. Lesieur, Parameterization of small scales of the three-dimensional isotropic turbulence utilizing spectral closures, J. Atmos. Sci. 38 (1981) 2747–2757.

[39] M. Lesieur, Turbulence in fluids, 4th Edition, Springer, 2008.

[40] C. W. Hirt, Computer studies of time-dependent turbulent flows, Phys. Fluids 12 (12) (1969) II–219–II–227.

[41] L. G. Margolin, W. J. Rider, Numerical regularization: the numerical analysis of implicit subgrid models, in: F. F. Grinstein, L. G. Margolin, W. J. Rider (Eds.), Implicit Large Eddy Simulation: Computing Turbulent Fluid Dynamics, Cambridge Univ. Press., 2007, pp. 195–221.

[42] E. Garnier, M. Mossi, P. Sagaut, P. Comte, M. Deville, On the use of shock-capturing schemes for large-eddy simulation, J. Comp. Phys. 153 (2) (1999) 273–311.

[43] R. Pasquetti, C. J. Xu, High-order algorithms for large-eddy simulation of incompressible flows, 17 (1) (2002) 273–284.

[44] T. Dairay, V. Fortuné, E. Lamballais, L. Brizzi, LES of a turbulent jet impinging on a heated wall using high-order numerical schemes, Int. J. Heat and Fluid Flow 50 (2014) 177–187.

[45] J. Smagorinsky, General circulation experiments with the primitive equations, Mon. Weath. Rev. 91 (3) (1963) 99–164.

[46] M. Germano, U. Piomelli, P. Moin, W. H. Cabot, A dynamic subgrid-scale eddy viscosity model, Phys. Fluids A 3 (7) (1991) 1760–1765.

[47] F. Nicoud, F. Ducros, Subgrid-scale stress modelling based on the square of the velocity gradient tensor, Flow Turb. Combust. 62 (3) (1999) 183–200.

[48] M. O. Deville, P. F. Fischer, E. H. Mund, High-order methods for incompressible fluid flow, Cambridge University press, 2002.

[49] G. Karniadakis, S. Sherwin, Spectral/hp Element Methods for Computational Fluid Dynamics, 2nd Edition, Oxford science publications, 2005.

[50] C. J. Xu, R. Pasquetti, Stabilized spectral element computations of high Reynolds number incompressible flows, J. Comp. Phys. 196 (2004) 680–704.

[51] R. Pasquetti, Spectral vanishing viscosity method for LES: sensitivity to the SVV control parameters, J. Turbulence 6 (12) (2005) 1–14.

[52] S. J. S. R. M. Kirby, Stabilisation of spectral/hp element methods through spectral vanishing viscosity: Application to fluid mechanics modelling, Comput. Methods Appl. Mech. Engrg. 195 (2006) 3128–3144.

[53] R. Pasquetti, Spectral vanishing viscosity method for large-eddy simulation of turbulent flows, Journal of Scientific Computing 27 (1–3) (2006) 365–375.

[54] R. Pasquetti, E. Séverac, P. Bontoux, M. Shäfer, From stratified wakes to rotorstator flows by an SVV–LES method, Theor. Comput. Fluid Dyn. 22 (2008) 261–273.

[55] E. Séverac, E. Serre, A spectral vanishing viscosity for the LES of turbulent flows within rotating cavities, J. Comp. Phys. 226 (2007) 1234–1255.

[56] S. Viazzo, S. Poncet, E. Serre, A. Randriamampianina, P. Bontoux, High-order large eddy simulations of confined rotor-stator flows, Flow Turb. Combust. 88 (2012) 63–75.

[57] J.-E. W. Lombard, D. Moxey, S. J. Sherwin, J. F. A. Hoessler, S. Dhandapani, M. J. Taylor, Implicit large-eddy simulation of a wingtip vortex, AIAA Journal In press (2015) 1–13.

[58] T. Hughes, L. M. K. Jansen, Large eddy simulation and the variational multiscale method, Computing and Visualization in Science 3 (1) (2000) 47–59.

[59] T. Hughes, L. Mazzei, A. Oberai, A. Wray, The multiscale formulation of large eddy simulation: Decay of homogeneous isotropic turbulence, Phys. Fluids 13 (2) (2001) 505–512.

[60] T. Hughes, A. Oberai, L. Mazzei, Large eddy simulation of turbulent channel flows by the variational multiscale method, Phys. Fluids 13 (6) (2001) 1784–1799.

[61] V. Gravemeier, The variational multiscale method for laminar and turbulent flow, Archives of Computational Methods in Engineering 13 (2) (2006) 249–324.

[62] D. Drikakis, C. Fureby, F. Grinstein, D. Youngs, Simulation of transition and turbulence decay in the Taylor-Green vortex, J. Turbulence 8 (20) (2007) 1–12.

[63] A. Aspden, N. Nikiforakis, S. Dalziel, J. Bell, Analysis of implicit les methods, Comm. App. Math. Comp. Sci. 3 (1) (2008) 103–126.

[64] D. Fauconnier, C. D. Langhe, E. Dick, Construction of explicit and implicit dynamic finite difference schemes and application to the large-eddy simulation of the Taylor-Green vortex, J. Comp. Phys. 228 (21) (2009) 8053–8084.

[65] D. Fauconnier, C. Bogey, E. Dick, On the performance of relaxation filtering for large-eddy simulation, J. Turbulence 14 (1) (2013) 22–49.

[66] J.-B. Chapelier, M. de la Llave Plata, F. Renac, E. Lamballais, Evaluation of a high-order discontinuous galerkin method for the dns of turbulent flows, Computers and Fluids 95 (2014) 210–226.

[67] Y. Zhou, F. F. Grinstein, A. J. Wachtor, B. M. Haines, Estimating the effective Reynolds number in implicit large-eddy simulation, Physical Review E 013303 (2014) 1–13.

[68] S. K. Lele, Compact finite difference schemes with spectral-like resolution, J. Comp. Phys. 103 (1992) 16–42.

[69] S. Laizet, E. Lamballais, High-order compact schemes for incompressible flows: a simple and efficient method with quasi-spectral accuracy, J. Comp. Phys. 228 (2009) 5989–6015.

[70] S. Laizet, E. Lamballais, J. C. Vassilicos, A numerical strategy to combine high-order schemes, complex geometry and parallel computing for high resolution DNS of fractal generated turbulence, Computers and Fluids 39 (3) (2010) 471–484.

[71] S. Laizet, N. Li, Incompact3d: a powerful tool to tackle turbulence problems with up to $o(10^5)$ computational cores, Int. J. Numer. Methods Fluids 67 (11) (2011) 1735–1757.

[72] A. G. Kravchenko, P. Moin, On the effect of numerical errors in large eddy simulation of turbulent flows, J. Comp. Phys. 131 (1997) 310–322.

[73] M. Germano, Turbulence : the filtering approach, J. Fluid Mech. 238 (1992) 325–336.

[74] D. K. Lilly, A proposed modification of the germano subgrid-scale closure method, Phys. Fluids A 4 (3) (1992) 633–635.

[75] E. Lamballais, V. Fortuné, S. Laizet, Straightforward high-order numerical dissipation via the viscous term for direct and large eddy simulation, J. Comp. Phys. 230 (2011) 3270–3275.

[76] V. Borue, S. A. Orszag, Local energy flux and subgrid-scale statistics in three-dimensional turbulence, J. Fluid Mech. 366 (1998) 1–31.

[77] N. E. Haugen, A. Brandenburg, Inertial range scaling in numerical turbulence with hyperviscosity, Physical Review E 70 (2) (2004) 1–7.

[78] A. G. Lamorgese, D. A. Caughey, S. B. Pope, Direct numerical simulation of homogeneous turbulence with hyperviscosity, Phys. Fluids 17 (1) (2005) 1–10.

[79] E. Tadmor, Convergence of spectral methods for nonlinear conservation laws, SIAM J. Numer. Anal. 26 (1) (1989) 1–30.

[80] Y. Maday, E. Tadmor, Analysis of the spectral vanishing viscosity method for periodic conservation laws, SIAM J. Numer. Anal. 26 (4) (1989) 854–870.

[81] G.-S. Karamanos, G. E. Karniadakis, A spectral vanishing viscosity method for large-eddy simulations, J. Comp. Phys. 163 (11) (2000) 22–50.

[82] A. N. Kolmogorov, Kolmogorov, A. N. (1991). Dissipation of energy in the locally isotropic turbulence, Dokl. Akad. Nauk SSSR 32 (1).

[83] Y.-H. Pao, Structure of turbulent velocity and scalar fields at large wavenumbers, Phys. Fluids 8 (6) (1965) 1063–1075.

[84] A. N. Kolmogorov, The local structure of turbulence in an incompressible fluid with very large reynolds numbers, Dokl. Akad. Nauk SSSR 30 (1941) 301–305.

[85] S. Goto, J. Vassilicos, Local equilibrium hypothesis and taylor's dissipation law, Fluid Dynamics Research 48 (2).

[86] M. Brachet, D. Meiron, S. Orszag, B. Nickel, R. Morf, U. Frisch, Small-scale structure of the Taylor-Green vortex, J. Fluid Mech. 130 (1983) 411–452.

[87] U. Frisch, S. Kurien, R. Pandit, W. Pauls, S. S. Ray, A. Wirth, J.-Z. Zhu, Hyperviscosity, Galerkin truncation, and bottlenecks in turbulence, Physical Review Letters 101 (14) (2008) 1–4.

[88] C. Cichowlas, P. Bonaïti, F. Debbasch, M. Brachet, Effective dissipation and turbulence in spectrally truncated Euler flows, Phys. Rev. Lett. 95 (264502) (2005) 1–4.